ABSTRACT

AN ANALYTICAL AND EXPERIMENTAL STUDY OF THE THERMAL SPECTRAL PROPERTIES OF OXIDE-METAL COMPOSITE MEDIA

by Syed Abdullah Hassan

The purpose of this study was to determine the corrosion rates of zinc and galvanized steel and to relate their optical properties to the amount of corrosion in the radiation spectrum of 0.35 to 2.75 micron wavelengths from a 10,000^{o}R source (sun) and a 3000^{o}R source (tungsten lamp).

Samples of zinc and galvanized steel were corroded for several durations up to 3 months in outdoor atmosphere and up to 4 weeks in a spray cabinet using a continuous spray of water. The corrosion film thicknesses were measured by the weight-change method (removal of the corrosion products from the test surface), by the x-ray diffraction method and by the metallographic method.

A Beckman DK-1A ratio recording spectrophotometer with a Beckman 24500 reflectance attachment was used to measure the hemispherical reflectance at normal incidence in the wavelength range 0.35 to 2.75 microns. The hemispherical reflectance curves so obtained were normalized with the energy distribution curves of the 10,000^{o}R and 3000^{o}R sources to obtain the corresponding integrated hemispherical reflectance curves. The average of these

curves, called mean integrated hemispherical (MIH) reflectance, were used as a criterion for the optical behavior of the samples.

The corrosion films produced in the atmosphere were smoother than those produced in the spray cabinet. The film thicknesses varied from 1.2 to 12.6 microns. The rate of corrosion was appreciable for the first 2 weeks in the atmosphere and the first two days in the spray cabinet. In the remaining period the rate was relatively small.

The MIH reflectance decreased with the growth of the corrosion films. For the 10,000^{o}R source nearly 75% of the reduction occurred in films 3.0 microns thick, but for the 3000^{o}R source the rate was relatively constant at all thicknesses. The corresponding increase in MIH absorptance was 76% for the 10,000^{o}R source and 117% for the 3000^{o}R source.

The experimental values of MIH reflectance were correlated with the theoretical predictions based on the Maxwell's theory of wave propagation through stratified media (assumed perfectly smooth) using a value of .0017 for the extinction coefficient of zinc oxide corrosion film. The agreement was good at large film thicknesses but was poor for films less than 4.0 microns thickness. This was attributed to the fact that the effect of surface roughness, which was neglected in the theoretical analysis, was in fact proportionately large at small film thicknesses.

The MIH reflectance showed at least a qualitative correlation with the surface roughness. The trends of the curves were comparable with those reported in the literature. The separate effects of the film thickness and the surface roughness, however, could not be ascertained in this study because of the simultaneous and uncontrolled variations of these factors.

Approved Fred H. Bulow
Major Professor

Approved Carl W. Hall
Department Chairman

AN ANALYTICAL AND EXPERIMENTAL STUDY OF THE THERMAL SPECTRAL PROPERTIES OF OXIDE-METAL COMPOSITE MEDIA

By

Syed Abdullah Hassan

A THESIS

Submitted to
Michigan State University
in partial fulfillment of the requirements
for the degree of

DOCTOR OF PHILOSOPHY

Department of Agricultural Engineering

1966

To

Mr. and Mrs. Mohsin Shah Bokhari

Syed Jafar Hassan

ACKNOWLEDGEMENTS

I would like to extend my very sincere appreciation to Dr. F. H. Buelow (Agricultural Engineering) for his inspiring guidance during my graduate program.

I am especially thankful to Dr. A. M. Dhanak (Mechanical Engineering) for his valuable suggestions and active interest in my work. I benefited greatly from his expert knowledge of the area of radiant heat transfer.

My sincere thanks are due to Dr. C. W. Hall (Agricultural Engineering) and Dr. Herman Rubin (Statistics) for serving on my guidance committee.

I am also indebted to Dr. D. E. Scherpereel (Metallurgy, Mechanics and Materials Science) for help in the x-ray and metallographic studies and Mr. Wayne Fredricks (State Highway Laboratories) for use of the spectrophotometer. Assistance of Mr. James Cawood and his staff in the Agricultural Engineering Research Laboratory is thankfully acknowledged.

TABLE OF CONTENTS

LIST OF FIGURES

LIST OF APPENDIX TABLES

INTRODUCTION

The present day reserves of fossil fuels are being depleted very rapidly. To meet the ever increasing demands for energy, need has grown to find new sources which can provide energy at competitive cost and in large quantities. Use of solar energy has been investigated very widely in the last twenty years. Whereas some of the applications like water heating, crop drying, and solar cooking are already competitive and are in mass use, other applications need further improvements in design and efficiency before they can replace the conventional sources.

On a bright summer day (assuming 8 hours of sunshine) a 100 square meter surface receives about 2.0×10^6 BTU's per day of solar energy (Daniels, 1955), which is roughly equivalent to 150 pounds of soft coal or 250 pounds of wood per day.

Despite the great abundance, solar energy suffers from a disappointingly low intensity level, which in most applications must be increased at the expense of efficiency. Therefore best prospects for utilization of solar energy lie in applications requiring low grade heat where the solar energy can be used directly without concentration. Morse and Dunkle (1962) estimated that by 1977 the per capita energy demand will increase from 0.36 to 0.47 equivalent

metric tons of coal per annum, more than half of which will be used as low grade heat. If solar energy were to supply half of this, the fuel savings would amount to the equivalent of one hundred million metric tons per annum.

The aforementioned water heating, drying of agricultural products and space heating are some of the low grade heat applications in point. Mass produced solar water heaters are already in domestic use in Australia, Israel, and Japan and provide hot water more economically than electric heaters (Morse, 1962, Sabotka, 1961, Tanishita, 1961). Hay and grain have been dried successfully using a solar heat supplemented forced air drying system (Buelow, 1961, Davis and Lipper, 1961). Air flow rates of ten to fifteen cubic feet per minute per square foot of collector were used, producing a temperature rise of ten to twenty degrees Fahrenheit which reduced the drying time of the products to less than half.

When utilized as a supplemental source, the solar energy is used only as available, thereby eliminating the need for a heat storage (Buelow, 1956, Sabotka, 1961). A simple and inexpensive absorber design may be used to absorb solar energy. A typical solar heater used for space heating or crop drying consists of a metallic surface provided with an air duct at the back. The air, heated by the metal surface during its passage through the duct, is subsequently used in the desired application.

Since the performance of the system depends on the ability of the metal surface to absorb incident solar radiations which lie in the wavelength range of 0.3 to 2.5 microns, efforts have been made to find new materials with good absorption in this range and to treat the existing materials so as to improve their absorption characteristics (Duffie, 1961).

Coating the absorber surface with a non-selective black (or dark) paint of high absorptivity is one of the oldest and most widely used methods. More recently, however, selective surfaces have been used (Edwards, 1961, Tabor, 1961, Trombe, 1961, Close, 1961) which exhibit high absorptivity in the solar spectrum and low emissivity at longer wavelengths (thus reducing loss with long wavelength radiations emitted at the surface temperature). The selective surfaces are formed by coating, folding, grooving or etching (Duffie, 1961). Selective coating of nickel black on galvanized steel (solar radiation absorptivity 0.89 and emissivity 0.12 at temperatures less than one hundred degrees Celcius) and Ebonol C on copper (α = 0.91, ϵ = 0.16) are already in commercial production for use in solar water heating and optical applications respectively (Tabor, 1961, Edwards, 1961).

The treated surfaces (selective and painted) suffer from one or more of the following inherent disadvantages:

1. High cost of initial treatment.
2. Unattractive appearance.

3. Recurring expenses in maintenance.
4. Greater resistance to heat transfer through the absorber surface owing to poor conducting coating or paint layer.
5. Gradual deterioration of absorption properties of the coated surface.

Untreated metal surfaces, on the other hand, improve their initially low absorption properties with time. When exposed to the atmosphere during use, a thin film of corrosion products (oxide) is formed on the metal surface which increases its absorption owing to multiple reflections in the film (Born, 1964, Duffie, 1961). In addition, the surface does not require extensive maintenance and is a good conductor of heat.

Even though corrosion starts a destructive process on the metal surface, metals most commonly used in solar heaters (galvanized steel and zinc) form protective layers. The layers formed first protect the underlying base metal and consequently retard the further rate of corrosion.

It is therefore of interest to investigate the behavior of untreated absorber surfaces in regard to both their radiation properties and corrosion (oxide) layer development.

Objectives

This study was undertaken with the following objectives:

1. To determine the thickness of corrosion (oxide) films of zinc and galvanized steel as a function of time.
2. To determine the spectral radiation properties of zinc and galvanized steel in the wavelength range of 0.35 to 2.75 microns at various film thicknesses.

REVIEW OF LITERATURE

A review of the literature on the corrosion behavior and the optical properties of zinc (and other metals) reveals two facts:

1. Extensive work has been done by chemists on the corrosion of zinc (and other metals), explaining the mechanism of corrosion, the rate of layer build-up and the influence of various factors.
2. Equally elaborate work is reported by physicists on the optical properties of "thin films" of evaporated metals and metal compounds and thermal oxides (produced by heating in air).

Yet no effort has been made by either group to study the growth of relatively "thick" corrosion films on metals and simultaneously investigate the associated changes in the optical properties. Very recently, however, interest has grown in this area because of the demands of aerospace applications for information on thermal radiation properties of coatings used as heat shields and selective coatings used on satellites. The first reference cited below is a case in point.

Francis and Love (1966) investigated the radiant behavior of isothermal absorbing coatings on conductors by solving the transport equations across the coating using

what they called the "attenuated intensity" and the "attenuated flux" approaches. They obtained plots of monochromatic absorptivity and emittance of aluminum, copper, nickel, gold and silver into absorbing coatings with a range of refractive indices and several thicknesses (from 0.075 to 0.600 micron (μ)). These curves show that as the optical thickness (refractive index times the geometrical thickness) of the absorbing coating was increased the emittance became more nearly that of a dielectric. At small angles the directional emittance into the coating was found to be greater than into the air. The attenuated flux and the attenuated intensity approaches yielded different results. This was explained by the fact that the attenuated flux approach could not "detect" the directional variations of the intensity.

Hall and Ferguson (1955) measured reflectance and transmittance of several evaporated ZnS films (on non-absorbing glass and rock salt substrates) ranging in thickness from 1 to 4 μ in the spectral region of 0.6 to 14 μ. Substituting these values into the theoretical equations, they calculated the absorption coefficient k and the spectral values of the refractive index n. The absorption coefficient was found to be approximately 0.001 and the refractive index ranged from 2.34 at 0.6 μ to 2.15 at 14 μ.

Hass and Salzburg (1954) prepared evaporated films of pure SiO in thicknesses ranging from 0.033 to 1.950 μ, which were later oxidized to SiO_2 by heating in air at 800

degrees Celsius. A comparison of the absorption curves of pure SiO films and the oxidized (SiO_2) films in the range 0.24 to 14 μ showed that the ten micron absorption peak, characteristic of SiO, shifted toward shorter wavelengths and the total absorption was increased.

Sennett and Scott (1950) obtained reflectance curves for evaporated films of eight different metals with thicknesses varying from 0.003 to 0.05 μ. For a monochromatic wave of 0.6 micron the absorptance of chromium, palladium, nickel and antimony films increased from zero at zero film thickness to between 0.40 and 0.55 for a 0.06 μ thick film. The rate of film evaporation was observed to affect both the film structure and the optical properties. Slow rates, in general, produced a more aggregated structure and increased absorption.

Scott (1955) stated that the optical constants of thin metal films may differ radically from those of the bulk metals. Bock (1945) observed that the curves of the electrical conductivity (which determines the reflection behavior) of evaporated zinc films in the range 0.48 to 2.4 μ were identical in shape with those reported for bulk zinc, but the absolute values were only about half.

Surface Roughness

It is well known that the surface roughness influences the reflection behavior of materials. A published account of this fact can be traced back 50 years. However, it was

not until a few years ago that a rigorous mathematical analysis of this effect was presented.

Except for Agnew and McQuiston (1953) who worked with powders, most of the studies are concerned with metallic surfaces. A general concensus of the reported work indicates that:

1. The influence of surface roughness σ is more pronounced in the short wavelength region (especially for large values of σ/λ) than in the long wavelength region.

2. The influence is greater for small incidence angles than for large incidence angles.

3. The surface roughness is much more critical in specular reflectance studies than in total reflectance studies.

In 1916 Gorton (1916) conducted experiments with electroplated ground glass samples to investigate the effect of surface roughness on the specular reflectance at several incidence angles in the spectral range 0.6 to 14.0 μ. His experiments showed that the specular reflectance was independent of surface roughness at long wavelengths, particularly at large incidence angles. It was, however, strongly influenced by the surface conditions at short wavelengths and small angles of incidence.

Three years later, based on the assumptions that the distribution of surface irregularities follow the probability law and that "the relative reflection of a rough surface depends only on its topography and not upon the nature of

the material of which it is composed", Chinmayanandam (1919) devised a mathematical equation describing the effect of surface roughness, which was found to be in general agreement with the experimental results of Gorton (1916) for moderate angles. For large angles from perpendicular, however, the agreement was poor. For these angles he suggested an empirical equation with constants calculated from Gorton's data.

More recently, Bennett and Porteus (1961) obtained an expression for $\sigma \ll \lambda$, based on the diffraction theory and Davies (1954) statistical approach relating the measured reflectance R (which includes both specular and diffuse reflectance) with surface roughness σ and slope m at normal incidence and for instrument acceptance angle $\Delta\theta$.

$$R = R_o \, e^{-\left(\frac{4\pi\sigma}{\lambda}\right)^2} + R_o \, \frac{32\pi^2}{m^2} \left(\frac{\sigma}{\lambda}\right)^4 (\Delta\theta)^2$$

This expression suggested that the specular reflectance which is given by the first term was predominant in the long wavelength region (or small σ/λ) whereas the diffuse reflectance given by the second term was prevalent in the short wavelength region (or large σ/λ).

Aluminized samples of steel and ground glass were used to measure reflectance as a function of surface roughness (0.07, 0.2 and 0.81 μ) in the wavelength range 2-22 μ. The results were found to be in excellent agreement with the theoretical equation in the wavelength region 5-22 μ. Below

5 μ, however, large discrepancies existed which were explained as due to the violation of the basic assumption that $\sigma \ll \lambda$.

Porteus (1963) later extended the analysis to the short wavelength region highlighting the restrictions on application to surfaces with peculiarities. Bennett (1963) tested the theory using aluminized ground glass samples. He suggested that the theory could be used to determine the height distribution of surface irregularities at sufficiently short wavelengths.

Birkebak et al (1964) investigated the roughness dependence of hemispherical and specular reflectance of ground nickel samples at several incidence angles using a black body radiation source at different temperatures. They found that the hemispherical reflectance was independent of surface roughness beyond a certain roughness value (0.4-0.8 μ) but the specular reflectance decreased steadily with increasing roughness. The hemispherical reflectance was also independent of incidence angles whereas the specular reflectance increased with increasing angles. Both hemispherical and specular reflectances decreased with increasing source temperatures, the change being about 10% for the range of temperatures considered (170° - 660°F). Birkebak and Eckert (1965) later added aluminized ground glass samples to these studies which were extended to include biangular reflectance and hemispherical-angular reflectance measurements.

Corrosion of Zinc and Galvanized Steel

Atmospheric corrosion of zinc and galvanized steel depends primarily on the purity and surface condition of the metal, the presence of moisture and the extent of contamination of the atmosphere with dust and corrosive gases. Presence of moisture is by far the most important factor. Vernon (1935) found that the corrosion rate of zinc remains negligibly small below a critical humidity value of about 70%. Above this value, however, the rate increases with increasing relative humidity.

Atmospheric dust containing suspended particles of soils, salts, carbon and carbon compounds or metal oxides is present to some extent in all atmospheres. Kutzelnigg (Uhlig, 1963) reported that rural atmospheres contain, on the average, about 2 mg/cm^3 of dust whereas the industrial atmospheres may contain as much as 1000 mg/cm^3. When settled on a metal surface, the dust combines with the moisture present in the air and initiates corrosion by forming galvanic or differential aeration cells. To show the influence of atmospheric dust, Vernon (1935) compared the corrosion of screened and unscreened samples exposed indoors for several months. The screened samples were found free of rust whereas the unscreened samples showed considerable rust and weight gain.

Among the gases polluting the atmosphere, sulphur dioxide is most corrosive to zinc and galvanized steel. It is produced mainly from the burning of coal, oil and

gasoline (Evans, 1961). Seasonal variations of fuel consumption affect the content of sulphur dioxide and therefore the corrosiveness of the atmosphere. This was confirmed by Schikorr (Uhlig, 1963),who exposed zinc samples to Berlin and to Stuttgart atmospheres and found that the samples corroded more rapidly in winter than in summer.

Data on atmospheric testing of zinc and galvanized steel is available from a number of sources (Uhlig, 1948). However, the most widely accepted values are based on the 10 and 20 year tests of A.S.T.M. (1955), 10 year tests of the New Jersey Zinc Company (Uhlig, 1948) and 10 year tests of B.I.S.R.A. (Uhlig, 1948). The average reported values for different atmospheres are summarized below:

	ATMOSPHERE			
	Industrial mils/year	Marine mils/year	Rural mils/year	Desert mils/year
Zinc	0.210	0.048	0.040	0.008
Galvanized steel	0.270	0.120	0.090	--

Tests indicate that zinc and galvanized steel corrode slowly and uniformly without deep pitting at a rate governed by the composition of the surrounding atmosphere (Uhlig, 1948).

Zinc and galvanized steel form protective corrosion films which retard the rate of corrosion. Ellis (1949) found that the corrosion rate of zinc exposed for 28 days to an industrial atmosphere depended largely on humidity and moisture conditions during the first five days of exposure and less on conditions arising later.

Atmospheric tests closely approximating the service conditions provide a reliable method of predicting the behavior of metals in actual use. However, they require a long period of time before useful conclusions can be drawn. The need for an accelerated test which could produce compatible results in a short time is therefore apparent. Methods investigated so far include immersion tests, acidic tests, electrochemical tests, air conditioner tests and spray tests (Evans, 1961).

The spray testing method has been investigated very widely in the past 40 years both in Europe and in America (Evans, 1961). Intermittent or continuous sprays of pure water (B.I.S.R.A., 1948), 5% and 20% NaCl solutions (A.S.T.M., 1962), natural and artificial sea water, dilute sulfuric acid (I.S.I., 1931), and salt solution acidified with acetic acid (McMaster, 1956) have been tried to simulate accelerated conditions for different atmospheres. An excellent review of spray testing literature is presented by Voigt (1948) and in a critique by Evans (1961). Thus far this method has failed to become reproducible partly because of lack of thorough understanding of such influencing factors as the size and shape of spray nozzles, air-solution ratios, size and location of samples and the size of the spray box.

The American Society for Testing Materials has adopted a spray testing method (A.S.T.M. Designation B117-62) with the reservation that it "does not prescribe the type of test specimens or exposure periods to be used for a specific

product, nor the interpretation to be given to the results."

Preparation of Samples

As pointed out by Evans (1961), Meyers (1948), A.S.T.M. (1952), Jelinek (1959), Knapp (1948) and Gwyther (1947) it is essential to remove surface grease, oil, oxides and other contaminants from the test samples in order to obtain reproducible corrosion test results.

Surface preparation generally consists of a degreasing process followed by rust removal by abrasion, machining or pickling in an acidic solution (Evans, 1961). Wesley (1953) prepared alloy steel samples by removing 0.0003 inches off the surface by machining. Mulvaney (1962) used a pickling solution of 15% (by weight) hydrochloric acid with 0.4% (by volume) Rodine 213 inhibitor at 200^{o}F. McCollan and Warrick (1948) reported that wide variations are possible in pickling solutions and temperatures depending on the material of the samples, the character of the scales and the surface desired after pickling. Although the pickling method is preferred by many researchers, Evans (1961) pointed out that it may leave a hydrogen charge or an organic film when an inhibited acid is used.

A detailed account of the degreasing methods is given by Champion (1952) and Meyers (1948). Simple solvent cleaning, emulsifiable solvent cleaning and vapor degreasing are among the methods most commonly used. Different solvents are preferred by different workers. A partial list of

solvents includes acetone, benzene, xylene and carbon tetrachloride (Evans, 1961).

Weast and Shulman (1962) degreased the samples by successive washings in acetone, ammonium chloride solution and distilled water. Researchers at New Jersey Zinc Company (Uhlig, 1948) washed their samples with ether and alcohol. Mulvaney (1962) followed A.S.T.M.'s (1958) recommended procedure. He used successive washings in carbon tetrachloride solution, trichloroethylene vapor degreasing bath, alcohol, distilled water and finally acetone. Gwyther (1947) recommended the use of emulsifiable cleaners mixed with kerosine and subsequent rinsing with water.

Measurement of Film Thickness

The methods of film thickness measurements can be categorized as gravimetric, electrochemical and optical. The choice of a particular method will of course depend on the requirements of an individual situation.

Gravimetric methods of thickness measurements are based on the change in weight of the specimen on corrosion and are by far the most widely used methods in corrosion studies. The change in weight may be measured either with the corrosion film in place or after complete removal of the corrosion products from the sample surface. For zinc, Anderson (1946) reported that the only acceptable weight change data are those based on chemically cleaned samples. Data from samples weighed with the corrosion products in place are misleading.

According to Champion (1952) and Knapp (1948) the corrosion products may be removed mechanically (by scrubbing with a brush, abrasive or detergent), electrochemically (by making the specimen a cathode), or chemically (using various chemical reagents). Whatever the method, it must be capable of removing all the corrosion products without loss of the base metal.

Stroud (1951) used cold chromic acid containing silver and strontium chromate to remove corrosion products from zinc samples. He also tried ammonium acetate but found that it removes only thin layers. At New Jersey Zinc Company (Uhlig, 1948) a 10-minute immersion in 10% ammonium acetate at $88^{\circ} \pm 1^{\circ}C$ was used. Hudson (Evans, 1961) cleaned zinc samples first by removing loose products with a wooden scraper and then immersing in cold 10% acetic acid solution for 1 minute.

The electrochemical method consists of removing corrosion film by cathodic reduction at constant current. The completion of the process is indicated by a sharp shift in the E.M.F. Campbell and Thomas (1959) used this method to measure 0.002 μ to 0.1 μ thick oxide and mixed oxide-sulfide films on copper and silver. The method can be used even for very thin films. Eurof Davies (1957) detected a 0.0005 μ film on silver heated at $800^{\circ}C$. The method has mainly been used for films on silver, copper, and iron (Evans, 1961).

Optical methods include interferometric, polarimetric and metallographic methods of measurements. The interferometric methods are based on the observation of the interference colors or fringes which occur when the film thickness is an odd multiple of quarterwavelength (of the incident ray). Interference colors were used by Tamman,et al (Evans, 1961), Evans and Bannister (1929), Constable (1927) and Vermilea (1953) to measure thin oxide films produced by heating the metal in the air. The color scale must, however, first be calibrated with some other known method. For absorbing media a knowledge of the phase change at the two interfaces is essential. This method is unsuitable for aluminum and other metals of high reflectivity with films of low refractive index (Kelly, 1958). Hass (1949), Winterbottom (1946), Kelly (1958) and many others measured film thickness from interference fringes, a technique introduced and developed by Tolansky (1948). The method is both simple and accurate but requires smooth surfaces and interfaces.

For the polarimetric method the changes in amplitude and phase of a polarized light on reflection from a film-covered surface are used to calculate thickness. These calculations are however, laborious and demand a thorough understanding of the underlying theoretical basis (Evans, 1961). Reference of complete details may be found in the pioneering work of Tronstad (1932) at Trondheim Labs, later continued and improved by Winterbottom (1946). William and

Hayfield (1957), Leberknight and Lustman (1939) and others have used this method to measure oxide films. Here again as pointed out by Tronstad (1935) the method is limited to films which are fairly uniform both in thickness and optical density.

Microscopic and metallographic methods have been used extensively for measuring thickness of protective coatings on metals (Blum, 1948). The method involves viewing a prepared cross-section of the sample under a microscope or projecting it on the graduated screen of a metallograph. Heussner (Blum, 1948) has outlined the procedure for preparing the samples and the necessary precautions especially for soft metals like tin and zinc. The method is accurate to about $\pm$ 5% but requires lengthy preparation of samples.

Howells (1954) and Blum (1948) have reviewed methods which are used to measure thickness of protective metal-coatings. Whereas most of the techniques used are empirical (like Preece test, spot test, jet test, etc.), the x-ray diffraction method needs special mention. The intensity of an x-ray beam diffracted from a film-free metal surface is attenuated after deposition of the film. From the ratio of the two intensities and the known values of the mass absorption coefficients of both the film and the base metal, the film thickness can be calculated. The method can be used according to Friedman and Birks (Heavens, 1965) for films of thickness 0.1 to 100 μ. Behr (Howells, 1954)

used x-rays to measure tin plating thickness on sheet steel.

THEORETICAL ANALYSIS

When a clean metal is exposed to corrosive media a thin layer of corrosion products is formed on the surface. The radiation properties of the composite surface thus formed will differ from the original surface depending on the following factors:

1. The composition and the optical properties of the corrosion products.
2. The roughness of the corrosion film and the underlying metal surface.
3. The thickness of the corrosion film.

The composition of the corrosion products can be determined from the knowledge of the corroding atmosphere. Once the composition is known the optical properties can be calculated from the appropriate values of optical constants.

The influence of the roughness at the two interfaces (air-oxide, oxide-metal) and the multiple reflections within the film layer combine to form a very complex optical situation which is further complicated in corrosion process where the geometrical shape and the distribution of the roughness can neither be controlled nor easily determined.

In order to render this problem to mathematical analysis it is assumed that all surfaces are perfectly smooth (and therefore the effect of the surface roughness

is neglected). The simplified model so obtained can be investigated using Maxwell's theory of propagation of electromagnetic waves through stratified media (Born, 1964; Harris, 1951; Heavens, 1965; and Hilsum, 1954). It is further assumed that:

1. The interface boundaries are sharp.
2. The material media are homogeneous and isotropic.
3. The magnetic permeability μ is unity in the frequency range considered.
4. The electromagnetic radiations are plane, time-harmonic and linearly polarized with the electric vector normal to the plane of incidence (called transverse electric, "TE" wave).
5. There are no currents and charges present, i.e.,

$$\vec{j} = o \text{ and } \rho = o$$

In the analysis that follows equations are derived for three mathematical models.

1. A dielectric film surrounded by two dielectric media (air).
2. A dielectric film on absorbing substrate (in air).
3. An absorbing film on absorbing substrate (in air).

An electric charge in space creates a state of excitation in its vicinity called the electromagnetic field which is represented by an electric vector $\vec{E}$ and a magnetic induction vector $\vec{B}$. Vectors $\vec{E}$ and $\vec{B}$ and the associated quantities (magnetic vector $\vec{H}$, electric displacement vector $\vec{D}$ and electric current density vector $\vec{j}$) are related by Maxwell's equations.

$$\text{curl } \vec{H} - \frac{1}{c}\dot{\vec{D}} = \frac{4\pi}{c}\vec{j} \tag{1}$$

$$\text{curl } \vec{E} + \frac{1}{c}\dot{\vec{B}} = o \tag{2}$$

and

$$\text{div } \vec{D} = 4\pi\rho \tag{3}$$

$$\text{div } \vec{B} = o \tag{4}$$

where ρ = electric charge density = 0 (assumed).

And "material equations" are used to describe the effect of these fields on material objects.

$$\vec{j} = \sigma \vec{E} \tag{5}$$

$$\vec{D} = \epsilon \vec{E} \tag{6}$$

and

$$\vec{B} = \mu \vec{H} \tag{7}$$

where

σ = specific conductivity

ϵ = dielectric constant

and

μ = magnetic permeability

Substances for which $\sigma \neq o$ are called "conductors" and those for which σ is negligibly small are called "dielectrics" or "insulators." Therefore the electric and magnetic properties of dielectrics are completely defined in terms of ϵ and μ. The magnetic permeability is $\mu = 1$ for most materials especially in the optical frequency range. Materials for which $\mu \neq 1$ are called magnetic.

Consider a plane polarized transverse electric wave incident on a stratified media. If the direction of stratification is along z, and yz the plane of incidence then

$E_y = E_z = o = H_x$. Assuming time dependence e^{-iwt}, the Maxwell's equations reduce to:

$$\frac{\partial H_z}{\partial y} - \frac{\partial H_y}{\partial z} + i \frac{\epsilon w}{c} E_x = 0 \qquad i = \sqrt{-1} \qquad (8a)$$

$$\frac{\partial H_x}{\partial z} - \frac{\partial H_z}{\partial x} = o \qquad (8b)$$

$$\frac{\partial H_y}{\partial x} - \frac{\partial H_x}{\partial y} = o \qquad (8c)$$

and

$$i \frac{w\mu}{c} H_x = o \qquad (9a)$$

$$\frac{\partial E_x}{\partial z} - i \frac{w\mu}{c} H_y = o \qquad (9b)$$

$$\frac{\partial E_x}{\partial y} + i \frac{w\mu}{c} H_z = o \qquad (9c)$$

The above equations relate the field vectors by simultaneous differential equations. By the process of elimination, differential equations can be obtained representing each vector separately. When there are no currents and no charges (i.e., $\vec{j} = o \quad \rho = o$), we get

$$\frac{\partial^2 E_x}{\partial y^2} + \frac{\partial^2 E_x}{\partial z^2} + n^2 k_o^2 E_x = \frac{d(\log\mu)}{dz} - \frac{\partial E_x}{\partial z} \qquad (10)$$

where n = refractive index $= \sqrt{\epsilon\mu}$

and k_o = wave number in vacuo or reduced wave number = $\frac{w}{c} = \frac{2\pi}{\lambda_o}$.

A solution of (10) in the form $E_x(y,z) = Y(y)U(z)$ yields

$$E_x = U(z)e^{i(k_o\alpha y - wt)} \tag{11}$$

where U(z) is a function of z and may be complex. Similarly we can obtain

$$H_y = V(z)e^{i(k_o\alpha y - wt)} \tag{12}$$

$$H_z = W(z)e^{i(k_o\alpha y - wt)} \tag{13}$$

Eliminating w from equations (12), (13), (8a), (9b) and (9c), we get

$$U' = \frac{dU(z)}{dz} = i\, k_o \mu V \tag{14}$$

$$V' = \frac{dV(z)}{dz} = i\, k_o(\epsilon - \frac{\alpha^2}{\mu})U \tag{15}$$

and separating V and U respectively from equations (14) and (15)

$$\frac{d^2U}{dz^2} - \frac{d(\log \mu)}{dz} \cdot \frac{dU}{dz} + k_o^2 (n^2 - \alpha^2)U = o \tag{16}$$

$$\frac{d^2V}{dz^2} - \frac{d\left[\log (\epsilon - \frac{\alpha^2}{\mu})\right]}{dz} \cdot \frac{dV}{dz} + k_o^2 (n^2 - \alpha^2)V = 0 \tag{17}$$

Similar relations may be obtained for a transmagnetic ("TM") wave using the substitution rule based on the symmetry of the Maxwell's equations.

Since both U(z) and V(z) satisfy a second order differential equation, each may be expressed as a linear combination of two particular solutions U_1, U_2 and V_1, V_2.

Therefore from equations (14) and (15)

$$U_1' = i k_o \mu V_1 \qquad U_2' = i k_o \mu V_2$$

$$V_1' = i k_o (\epsilon - \frac{\alpha^2}{\mu}) U_1 \text{ and } V_2' = i k_o (\epsilon - \frac{\alpha^2}{\mu}) U_2$$

which give

$$V_1 U_2' - U_1' U_2 = o \quad \text{and} \quad U_1 V_2' - V_1' U_2 = o$$

Thus

$$\frac{d}{dz} (U_1 V_2 - U_2 V_1) = o$$

which implies that the determinant

$$D = \begin{vmatrix} U_1 & V_1 \\ U_2 & V_2 \end{vmatrix} = \text{constant} \tag{18}$$

Most convenient choice of particular solutions is

$$\left.\begin{aligned} U_1 &= f(z) & U_2 &= F(z) \\ V_1 &= g(z) & V_2 &= G(z) \end{aligned}\right\} \tag{19}$$

such that $f(o) = G(o) = o$ and $F(o) = g(o) = 1$ (20)

Then solutions $U(o) = U_o$ and $V(o) = V_o$ may be written as

$$U = FU_o + fV_o$$

$$V = GU_o + gV_o$$

$$\text{or} \quad \begin{pmatrix} U \\ V \end{pmatrix} = \begin{pmatrix} F(z) & f(z) \\ G(z) & g(z) \end{pmatrix} \begin{pmatrix} U_o \\ V_o \end{pmatrix} \tag{21}$$

$$\text{or} \qquad Q = N Q_o \tag{22}$$

Square matrix N is a constant since the determinant D in (18) is a constant. Actually "N" is unimodular as can be seen immediately at z = o.

Let us define

$$Q_o = M\,Q \tag{23}$$

which from equation (21) is

$$M = \begin{pmatrix} g(z) & -f(z) \\ -G(z) & F(z) \end{pmatrix} = \begin{pmatrix} m_{11} & m_{12} \\ m_{21} & m_{22} \end{pmatrix} \tag{24}$$

M is a unimodular matrix and is called the "characteristic matrix" of the stratified media. It relates the x and y components of the electric (or magnetic in case of a "TM" wave) vectors in the plane z = o to the components in an arbitrary plane of constant z. Knowledge of the characteristic matrix for any stratified medium determines the propagation of the electromagnetic wave through it.

Expressions for reflection and transmission coefficient can be derived in terms of the elements of the characteristic matrix, using the boundary condition that (when $\vec{j}$ = o and ρ = o) the tangential components of $\vec{E}$ and $\vec{H}$ are continuous across a surface of discontinuity. For the "TE" wave incident at angle θ_1 and transmitted at angle θ_ℓ, where subscript 1 refers to the first medium and "ℓ" to the last, we get reflection coefficient

$$r = \frac{(m_{11} + m_{12}\,p_\ell)\,p_1 - (m_{21} + m_{22}\,p_\ell)}{(m_{11} + m_{12}\,p_\ell)\,p_1 + (m_{21} + m_{22}\,p_\ell)} \tag{25}$$

and transmission coefficient

$$t = \frac{2\, p_1}{(m_{11} + m_{12}\, p_\ell)\, p_1 + (m_{21} + m_{22}\, p_\ell)} \qquad (26)$$

where $p_i = \sqrt{\frac{\epsilon_i}{\mu_i}}\ \cos\theta_i \qquad i = 1, \ell$

For the "TM" wave, the above expressions can be used by replacing p_i with q_i where

$$q_i = \sqrt{\frac{\mu_i}{\epsilon_i}}\ \cos\theta_i \qquad i = 1, \ell$$

Let us now investigate some particular cases.

1. **A Homogeneous Dielectric Film Surrounded by Two Dielectric Media.**

If the normal to the incident wave makes an angle θ with the direction of stratification, then

$$\alpha = n \cos\theta$$

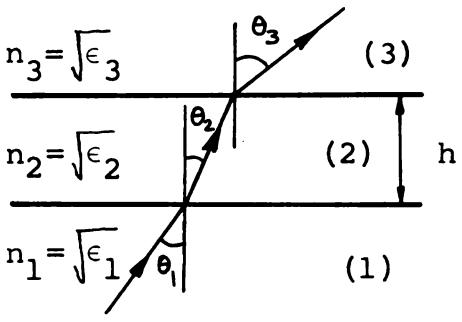

For an homogeneous medium ϵ and μ are constant (μ=1) and so the refractive index $n = \sqrt{\mu\epsilon} = \sqrt{\epsilon}$ is also constant. Therefore, the middle terms in equations (16) and (17) drop out and we get

$$\frac{d^2U}{dz^2} + (k_o^2\, n^2\, \cos^2\theta)\ U = o \qquad (27)$$

$$\frac{d^2V}{dz^2} + (k_o^2\, n^2\, \cos^2\theta)\ V = o \qquad (28)$$

which yield, subject to (14) and (15), the following solutions

$$U(z) = A \cos (k_o nz \cos \theta) + B \sin (k_o nz \cos \theta) \tag{29}$$

$$V(z) = \frac{1}{2}\sqrt{\frac{\epsilon}{\mu}} \cos \theta \left[B \cos (k_o nz \cos \theta) - A \sin (k_o nz \cos \theta) \right] \tag{30}$$

Using the boundary conditions given in equation (20), the particular solutions become

$$U_1 = f(h) = \frac{i}{p_2} \sin \beta$$

$$U_2 = F(h) = \cos \beta$$

$$V_1 = g(h) = \cos \beta$$

$$V_2 = G(h) = -i\, p_2 \sin \beta$$

where

$$\beta = k_o n_2 h \cos \theta_2 = \frac{2\pi}{\lambda_o} n_2 h \cos \theta_2$$

and

$$p_2 = \sqrt{\frac{\epsilon_2}{\mu_2}} \cos \theta_2$$

Therefore elements of the characteristic matrix are

$$\left.\begin{aligned} m_{11} &= \cos \beta & m_{12} &= -\frac{i}{p_2} \sin \beta \\ m_{21} &= i\, p_2 \sin \beta & m_{22} &= \cos \beta \end{aligned}\right\} \tag{31}$$

Therefore the overall reflection and transmission from equations (25) and (26) are

$$r = \frac{(p_1 \cos \beta - i \frac{p_1 p_3}{p_2} \sin \beta) - (p_3 \cos \beta - i\, p_2 \sin \beta)}{(p_1 \cos \beta - i \frac{p_1 p_3}{p_2} \sin \beta) + (p_3 \cos \beta - i\, p_3 \sin \beta)} \tag{32}$$

$$t = \frac{2p_1}{(p_1 \cos\beta - i\frac{p_1 p_3}{p_2}\sin\beta)+(p_3\cos\beta - i\, p_3 \sin\beta)} \quad (33)$$

The reflection and transmission coefficients for the two interfaces 1,2 and 2,3 can be obtained from the well known Fresnel's equation. For "TE" wave

$$r_{12} = \frac{n_1 \cos\theta_1 - n_2 \cos\theta_2}{n_1 \cos\theta_1 + n_2 \cos\theta_2} = \frac{p_1 - p_2}{p_1 + p_2} \quad (34)$$

since $p_i = \sqrt{\frac{\epsilon_i}{\mu_i}} \cos\theta_i = \sqrt{\epsilon_i}\cos\theta_i = n_i \cos\theta_i$ (for $\mu = 1$)

and

$$t_{12} = \frac{2\, n_1 \cos\theta_1}{n_1 \cos\theta_1 + n_2 \cos\theta_2} = \frac{2p_1}{p_1 + p_2} \quad (35)$$

Similarly

$$r_{23} = \frac{p_2 - p_3}{p_2 + p_3} \quad (36)$$

and

$$t_{23} = \frac{2p_2}{p_2 + p_3} \quad (37)$$

substituting from equations (34) to (37) in (32) and (33), it can be shown that

$$r = \frac{r_{12} + r_{23}\, e^{2\, i\beta}}{1 + r_{12}\, r_{23}\, e^{2\, i\beta}} \quad (38)$$

and

$$t = \frac{t_{12}\, t_{23}\, e^{2\, i\beta}}{1 + r_{12}\, r_{23}\, e^{2\, i\beta}} \quad (39)$$

Therefore

$$\text{Reflectivity } R = |r|^2 = \frac{r_{12}^2 + r_{23}^2 + 2\, r_{12}\, r_{23} \cos 2\beta}{1 + r_{12}^2\, r_{23}^2 + 2\, r_{12}\, r_{23} \cos^2\beta} \qquad (40)$$

and transmissivity

$$T = \frac{p_3}{p_1}|t|^2 = \frac{n_3 \cos\theta_3}{n_1 \cos\theta_1} \frac{t_{12}^2\, t_{23}^2}{1 + r_{12}^2\, r_{23}^2 + 2\, r_{12}\, r_{23} \cos 2\beta} \qquad (41)$$

From equations (40) and (41) phase change, δ_r, of the wave may also be obtained.

$$\tan \delta_r = \tan(\arg r) = \frac{r_{23}(1-r_{12}^2) \sin 2\beta}{r_{12}(1 + r_{23}^2) + r_{23}(1 + r_{12}^2)\cos 2\beta} \qquad (42)$$

2. A Homogeneous Dielectric Film On An Absorbing Substrate In Air.

Formulae developed above for stratified dielectric (transparent) media can also be applied to the conducting (absorbing) media provided appropriate changes are incorporated.

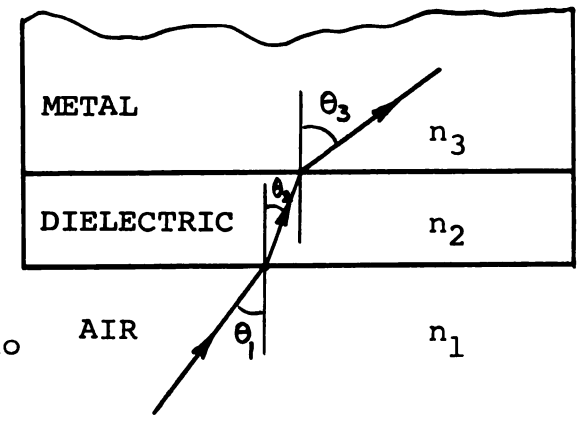

For absorbing media (metals, semi-conductors) the optical constants ϵ and n are no longer real but are complex quantities $\hat{\epsilon}$ and $\hat{n}$, given by

$$\hat{\epsilon} = \epsilon + i\,\frac{4\pi\sigma}{w} \qquad (43)$$

$$\hat{n} = n\,(1 + i\,K) \qquad (44)$$

K is called "extinction coefficient".

Formulae for dielectric media that involve only linear relation between the components of the field vectors of a time-harmonic wave can be used for the absorbing media on replacing ϵ, n, K etc. by $\hat{\epsilon}$, $\hat{n}$ and $\hat{K}$ as defined above.

If U_3 and V_3 are real quantities, we may write

$$\hat{n}_3 \cos \theta_3 = U_3 + i V_3 \tag{45}$$

and from the law of refraction

$$\hat{n}_3 \sin \theta_3 = n_2 \sin \theta_2 \tag{46}$$

Then from (45), (46) and (44) equating real and imaginary parts, we get

$$2 U_3^2 = n_3(1-K_3^2) - n_2^2 \sin^2\theta_2 + \sqrt{\left[n_3^2(1-K_3^2)-n_2^2\sin^2\theta_2\right]^2 + 4 n_3^4 K_3^2} \tag{47}$$

and

$$2 V_3^2 = -\left[n_3^2(1-K_3^2)-n_2^2\sin^2\theta_2\right] + \sqrt{\left[n_3^2(1-K_3^2)-n_2^2\sin^2\theta_2\right]^2 + 4 n_3^4 K_3^2} \tag{48}$$

Fresnel's equation (34) for a "TE" wave may now be written for absorbing media as

$$r_{23} = \rho_{23} e^{i\Phi_{23}} = \frac{n_2 \cos \theta_2 - \hat{n}_3 \cos \theta_3}{n_2 \cos \theta_2 + \hat{n}_3 \cos \theta_3} = \frac{n_2 \cos \theta_2 - (U_3 + 2 V_3)}{n_2 \cos \theta_2 + (U_3 + i V_3)} \tag{49}$$

where ρ_{23} is the amplitude ratio and Φ_{23} the phase change. From (49) the following is obtained on separating real and imaginary parts.

$$\rho_{23}^2 = \frac{(n_2 \cos \theta_2 - U_3)^2 + V_3^2}{(n_2 \cos \theta_2 + U_3)^2 + V_3^2} \tag{50}$$

and

$$\tan \Phi_{23} = \frac{2 V_3 n_2 \cos \theta_2}{U_3^2 + V_3^2 - n_2^2 \cos^2 \theta_2} \tag{51}$$

The overall reflection coefficient r can be derived from equation (38) on replacing r_{23} by $\rho_{23} e^{i\Phi_{23}}$. Thus

$$r = \frac{r_{12} + \rho_{23} e^{i(\Phi_{23}+2\beta)}}{1 + r_{12} \rho_{23} e^{i(\Phi_{23}+2\beta)}} \tag{52}$$

We observe that equation (52) is identical to (38) with ρ_{23} replacing r_{23} and $(\Phi_{23} + 2\beta)$ replacing (2β). Making this substitution in (40) and (42) we obtain net reflectivity and phase change. Thus

$$R = \frac{r_{12}^2 + \rho_{23}^2 + 2 r_{12} \rho_{23} \cos (\Phi_{23} + 2\beta)}{1 + r_{12}^2 \rho_{23}^2 + 2 r_{12} \rho_{23} \cos (\Phi_{23} + 2\beta)} \tag{53}$$

and

$$\tan \delta_r = \frac{\rho_{23} (1 - r_{12}^2) \sin (\Phi_{23} + 2\beta)}{r_{12} (1 + \rho_{23}^2) + \rho_{23} (1 + r_{12}^2) \cos (\Phi_{23} + 2\beta)} \tag{54}$$

3. An Absorbing Film Over An Absorbing Substrate In Air.

In this case the Fresnel's coefficients for both interfaces (1,2 and 2,3) involve complex quantities since

both the film and the substrate are absorbing. The equations may be written in the form

$$r_{12} = \frac{n_1 \cos\theta_1 - \hat{n}_2 \cos\theta_2}{n_1 \cos\theta_1 + \hat{n}_2 \cos\theta_2} = g_1 + i\, h_1 \qquad (55)$$

$$r_{23} = \frac{\hat{n}_2 \cos\theta_2 - \hat{n}_3 \cos\theta_3}{\hat{n}_2 \cos\theta_2 + \hat{n}_3 \cos\theta_3} = g_2 + i\, h_2 \qquad (56)$$

Equating real and imaginary parts in equation (44) and the above, we get for Normal Incidence,

$$g_2 = \frac{n_1^2 - n_2^2 - (n_2K_2)^2}{(n_1 + n_2)^2 + (n_2K_2)^2}, \quad h_2 = \frac{2\, n_1\, n_2\, K_2}{(n_1 + n_2)^2 + (n_2K_2)^2}$$

and

$$g_3 = \frac{n_2^2 - n_3^2 + (n_2K_2)^2 - (n_3K_3)^2}{(n_2 + n_3)^2 + (n_2K_2 + n_3K_3)^2}, \quad h_3 = \frac{2\, n_2 n_3 (K_3 - K_2)}{(n_2+n_3)^2 + (n_2K_2+n_3K_3)^2}$$

Using boundary conditions at the discontinuities, elements of the characteristic matrices expressed in terms of the Fresnel's coefficients are obtained. Substituting these in equations of the form (25) and after a lengthy simplifying process, the net reflectivity R for Normal Incidence is given by

$$R = \frac{(g_2^2+h_2^2)e^{2K_2\beta_2} + (g_3^2+h_3^2)\, e^{-2K_2\beta_2} + A \cos 2\beta_2 + A \sin 2\beta_2}{e^{2K_2\beta_2} + (g_2^2+h_2^2)(g_3^2 + h_3^2)e^{-2K_2\beta_2} + c \cos 2\beta_2 + D \sin 2\beta_2} \qquad (57)$$

where

$$A = 2\,(g_2g_3 + h_2h_3) \qquad B = 2\,(g_2h_3 - g_3h_2)$$

$$c = 2\,(g_2g_3 - h_2h_3) \qquad D = 2\,(g_2h_3 + g_3h_2)$$

and

$$\beta_i = \frac{2\pi\ n_i^*\ h}{\lambda_o} \cos\ \theta_i = \frac{2\pi\ n_i^*\ h}{\lambda_o} \qquad \text{(for normal incidence)}$$

The monochromatic reflectivity values for any of the three models considered can be calculated by substituting the monochromatic values of the optical constants n and K (for each media) in the appropriate equations. The three media used in this study were air, zinc oxide (corrosion film) and zinc (substrates).

EXPERIMENTAL PROCEDURE AND EQUIPMENT

The main phases in the experimental procedure were:

1. Preparation of samples.
2. Reflection measurements, before and after exposure.
3. Exposure to corroding atmospheres.
4. Measurement of surface roughness and film thickness.

The materials used in this study were specially requested from the manufacturers. Commercial quality rolled zinc (purity 99.6+%) made according to A.S.T.M. specifications B 69 - 39, type I was received from Matthiessen and Hegeler Zinc Company, LaSalle, Illinois and hot rolled galvanized steel A.S.T.M. designation A - 526 - 64T (0.0017 inch zinc coating) from Midwest Steel Division, National Steel Corporation, Portage, Indiana. These were wrapped in moisture proof packing immediately after manufacture to prevent weathering prior to tests.

1-1/2" x 2" size samples were cut from the zinc roll and the galvanized steel sheets. Effort was made to obtain the samples from as few sheets as possible so as to minimize variations among samples due to the material.

Using a vibrating stylus, the samples were marked at the top left hand and the bottom right hand corners for identification. In all 26 samples each of zinc and galvanized steel were used in the tests; eight with duplicates for the

atmospheric test and ten for the cabinet test. The scheme of exposure is given below:

Atmospheric test: 3, 7, 14, 21, 28, 42, 56, and 84 days

Cabinet test: 1/4, 1/2, 1, 2, 3, 5, 9, 14, 21 and 28 days

The samples were degreased by brushing lightly in a bath containing one part commercial emulsifier (Gunk) and three parts kerosine oil (Gwyther, 1947). They were left in the bath for about 5 minutes to allow penetration of solvent into the soil. The samples were then washed under running water, dipped in acetone to remove water from the surface and dried in a desiccator. Samples thus cleaned supported a continuous film when rinsed with cold water, indicating complete removal of grease, oil and soils from the surface (Gwyther, 1947).

Degreased samples are generally pickled to remove surface scales. To study the effects of pickling on zinc and galvanized steel, duplicate samples were pickled in a solution containing 2.0% HCl and 0.02% Rodine 213 (by weight) for 2 minutes at a temperature of 150^{o}F (Mulvaney, 1962). Based on the decrease in weight, average film removal was less than 0.05 microns for both zinc and galvanized steel. More significant, though, was the fact that pickling dulled the surface of the specimens thereby changing its reflection characteristics. For this reason it was decided not to pickle the samples.

The dried samples were weighed in a "Mettler" analytical balance with an accuracy of $\pm$ 0.00005 grams. The zero adjustment of the scale was checked before and during

each set of measurements. Specimen weight was indicated on a vernier scale to 0.0001 grams.

Total Reflectance Measurements

Since a suitable instrument was not available on the campus, facilities of the Michigan State Highway Laboratories in Lansing were used for reflectance measurements.

A Beckman DK - 1A ratio recording spectrophotometer with Beckman 24500 reflectance attachment (Figure 1) was used to obtain total reflectance curves at normal incidence in the wavelength range 0.35 to 2.75 microns for each sample before and after exposure. Hemispherical reflectance (also called total reflectance) includes both the specular and the diffuse reflectance. Therefore an integrating sphere (in the reflectance unit) is employed to direct all reflected beams from the sample (and the reference) onto the detector. A shift plate is used at the sample (and the reference) port which positions the sample (and the reference) at an angle of 5^{o} to the incident beam, so that the specularly reflected beam is also intercepted by the integrating sphere.

Ratio recording technique is based on the comparison of the beam energy from the sample to the beam energy from a standard reference. The method thus eliminates errors due to source fluctuations, changes in amplifier gain, variation in detector sensitivity or spectral response, and presence of absorbing gases in the beam paths.

Figure 4 shows the optical diagram for reflectance studies. A beam of light from a tungsten ($3,000^{o}R$) source

Figure 1. Beckman DK-1A spectrophotometer with reflectance attachment.

Figure 2. "Norelco" x-ray diffraction unit with recorder.

Figure 3. Balphot Metallograph with camera attachment.

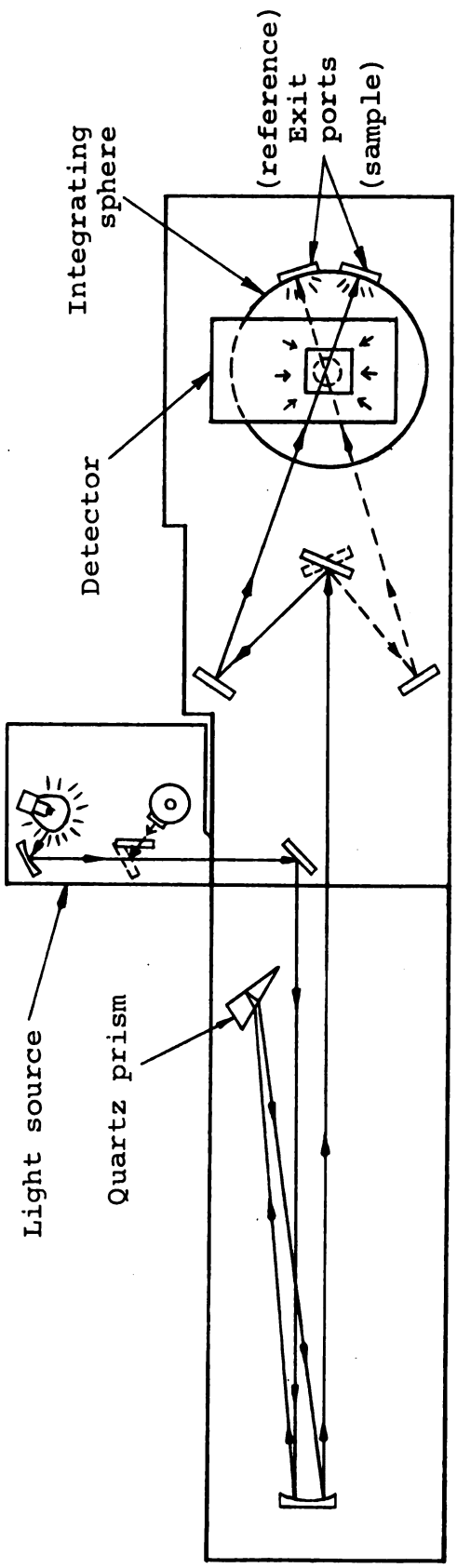

Figure 4. Light path in Beckman DK-1A spectrophotometer for hemispherical reflectance measurements.

is resolved on passing through a high-dispersion quartz prism. Using accurately adjustable slits, monochromatic beams are obtained. Slit width is automatically adjusted to maintain a relatively constant beam energy level. The monochromatic beam is then chopped into alternate reference beam and sample beam to provide a double beam system within the sample compartment. Both sample and reference beams are integrated, detected and amplified by the same components, and the ratio recorded on the chart. A combination of any one of the seven wavelength scanning rates and four separate chart speeds can be used. Manufacturer's indicated accuracy for reflectance measurements is $\pm$ 2% depending upon the accuracy of the reference standard.

A performance curve for barium sulphate, which was used as a reference standard, was obtained and the reflectance curves for the test specimens were corrected accordingly.

Exposure to Corroding Atmosphere

One set of eight samples, with duplicates, each of zinc and galvanized steel was exposed outside to the atmosphere and a second set of ten samples each was exposed to water spray inside a cabinet. Each sample was exposed for a predetermined duration and, once removed from the test, was not re-introduced.

Atmospheric Test

A wooden frame was built to hold the samples in four rows for exposure to the atmosphere. The top ends of the

specimens were clamped between the wooden frame and a clear plexiglass strip which was bolted down with winged nuts. This arrangement not only permitted easy withdrawal of samples but also provided an inert contact thereby preventing localized corrosion.

The frame was placed at an angle of 45° to the horizontal on the roof of a building south of the Agricultural Engineering building on the Michigan State University campus. In this position the samples were exposed unobstructed to the sun and the rain. The experiment was started on September 1, 1965.

Following the exposure scheme, duplicate samples were withdrawn from the frame, rinsed with water to wash off dust particles, dried and weighed. Reflectance curves were obtained and surface corrosion films measured by methods detailed later in this Chapter.

Cabinet Tests

A 2' x 3' x 2' size spray cabinet was built from plywood according to A.S.T.M. designation B 117 - 61, (Figure 5).Water spray in the form of fine mist was used as the corroding medium. To prevent water from soaking into the plywood, the inside of the cabinet was lined with heavy aluminum foil and covered with a plastic sheet. For the same reason, the spray water was stored in a plexiglass trough instead of directly in the cabinet as suggested in the designation.

Figure 5. Spray cabinet.

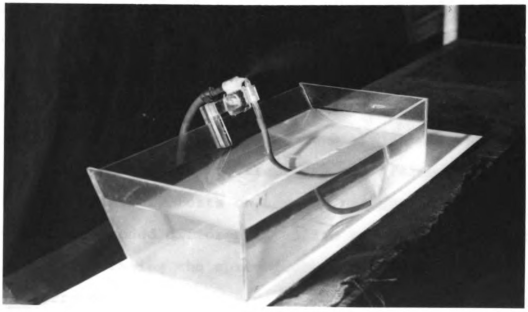

Figure 6. Air atomizing spray nozzle assembly.

An air atomizing spray nozzle assembly, as shown in Figure 6, was used to produce fine particle spray. The assembly consisted of two plexiglass nozzles (tube diameter 3/8" and nozzle opening 0.02" and 0.03" for air and water respectively) set at right angles to each other and mounted on a frame which easily attached to the trough. When mounted on the trough, the lower end of the vertical nozzle dipped well below the water surface and the horizontal nozzle was connected to an air supply regulated at 18 psi through a pressure regulating valve. The nozzles could be rotated in the vertical plane thus changing the angle of the spray. The spray was directed at the wall to arrest large size water droplets present in the spray.

The samples were held at the bottom between two plexiglass strips bolted together with winged nuts. The samples were so placed that they neither touched each other nor the clamping bolts. Three rows of strips were placed in the cabinet on supports 15" above the floor and 4" apart. The first support was about 6" to the side of the water trough. Thus the water dripping from the samples and the strips fell on the sloping floor and was drained out.

Preliminary tests on the cabinet showed that the specimens corroded differently on the two surfaces. In fact the surfaces facing the spray (rebounding from the wall) were corroded more vigorously and more evenly than the others. Therefore in the final experiment the test surfaces were placed facing the spray.

Water in the reservoir was replenished three to four times a day. The spray nozzles were cleaned periodically to remove precipitated solid deposits. The relative humidity inside the spray cabinet remained above 98% during the test and the temperature varied between 65° and 70°F.

Samples removed from the test were dried, weighed and then subjected to the reflectance and the corrosion film thickness measurements.

Measurement of Surface Roughness

Three measurements of surface roughness were made on each sample as outlined below:

1. Before exposure (clean, degreased surface).
2. After exposure with the corrosion products in place.
3. After removal of corrosion products.

These measurements gave the roughnesses of the clean metal surface, the oxide surface and the underlying corroded metal surfaces respectively.

A Micrometrical Profilometer type "QA" with Skidmount type "AA" was used to measure r.m.s. roughness values at 1/2" tracer stroke. The radius of the Skidmount was 0.000500" $\pm$ 0.000150. Manufacturer's indicated accuracy for the instrument was $\pm$ 2%.

Measurement of Corrosion Film Thickness

Average film thicknesses were calculated from the change in weight of the specimens on removal of the corrosion products from the test surface. In addition, metallographic

and x-ray diffraction methods were tried to investigate the feasibility of their application.

After getting the x-ray diffraction curves, the corroded samples were cut in half. One half was used in the metallographic method and the other in the weight-reduction method.

1. Weight-reduction method: A 10% acetic acid solution was used to remove the corrosion products (ZnO) from both zinc and galvanized steel samples (Evans, 1961). Since the corrosion products were to be removed from the test surface only, it was necessary to mask the back side. Preliminary tests with epoxy glue produced satisfactory results. Duplicate specimens of zinc and galvanized steel were coated on both sides and edges with epoxy glue and allowed to dry for a period of 12 hours. The samples were then weighed and dipped in 10% acetic acid solution for 2 minutes (twice the duration the test samples would be dipped for rust removal). They were then rinsed with water, dried in a desiccator for 6 hours and weighed. The average weight change in the specimens was observed to be less than 0.0003 grams. This would cause an error of less than 1% in the film thickness measurements.

The test samples were coated with epoxy glue on the back and the edges, dried for 12 hours and weighed. The samples were then dipped in a 10% acetic acid solution for 1 minute, scrubbing the surface with a nylon sponge. They were then rinsed with water, swabbed to remove excess water

from the surface and dried in a desiccator for 4 hours. Once again they were weighed and the reduction in weight was obtained by subtracting this weight from the first. Average film thickness h in microns was calculated from the formula

$$h = \frac{W}{AD} \times 10^4$$

where W = weight reduction in grams

A = surface area of the specimen in cm^2

D = density of the corrosion products in grams/cm^3

Since the samples were exposed to water spray inside the cabinet and a relatively pure atmosphere outside, it was assumed that the corrosion is primarily due to oxygen and that the surface rust is mainly ZnO. Therefore

$$h = \frac{W}{5.606A} \times 10^4 = 1783.803 \left(\frac{W}{A}\right) \text{ microns.}$$

2. Metallographic method: It involves projecting a polished cross-section of the sample onto a pre-calibrated graduated screen of the metallograph and reading the layer thickness directly from the screen. The method is laborious in that it requires a long and careful preparation of the samples.

The test samples were inbedded in cold plastic molds, commonly used in metallurgical studies, to prevent damage to the surface scale. Fine powder plastic was dissolved in a solvent to form a thin paste and was poured into a cylindrical ring placed over a flat aluminum plate. The plate surface as well as the interior of the ring was coated

with a thin layer of petroleum jelly to keep the plastic from sticking to these surfaces. A sample was then placed vertically in the middle of the ring and held in place until the plastic hardened (30 minutes). Four hours later it was removed from the form and wiped clear of excess grease.

The sample cross-section was then polished, first over three successive grades of emery cloth, and then three grades of polishing wheels. The sample was rotated through 90^{o} after each step to get better results. At the final polishing operation which used an abrasive of 1 micron particle size, the sample was polished across the width to enhance the demarkation of the boundaries.

A Balphot Metallograph (catalog No. 42 - 31 - 22) was used for thickness measurements, (Figure 3). Using a 20 x objective and a 10 x eyepiece, the image was projected on a ground glass plate at a bellow distance of 20". The plate can be replaced by a photographic film for taking pictures. The length of the cross-section was scanned in successive steps. An average film thickness was determined for each step. From these step-measurements, average film thickness was computed for the entire length of the cross-section.

3. X-ray diffraction method: A beam of x-rays refracted through a stratified media is attenuated according to the following law:

$$I = I_{o}\, e^{\left(-\frac{\mu}{\rho}\right)\rho x}$$

where I_o = intensity of the incident beam

I = intensity of the refracted beam

$(\frac{\mu}{\rho})$ = mass absorption coefficient

x = thickness of the medium

Thickness of oxide film in an oxide-metal composite medium can be calculated from the above equation by redefining the quantities as follows

I_o = intensity of beam refracted through "clean" metal

I = intensity of beam refracted through corroded metal (oxide + metal)

$(\frac{\mu}{\rho})$ = mass absorption coefficient of ZnO

x_f = oxide film thickness

$$x = \frac{x_f}{\cos\theta_i}$$

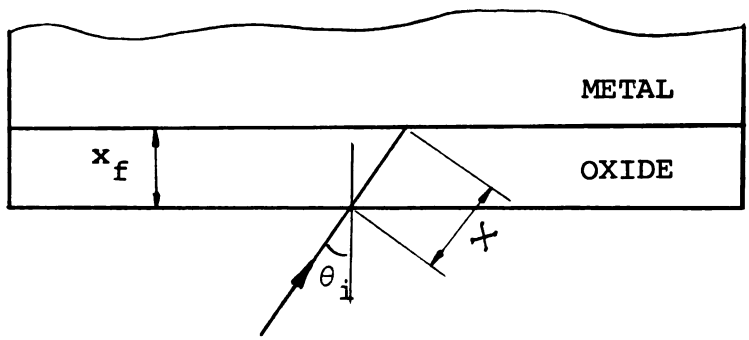

For better accuracy the measurements should be made at several "peak" values.

A "Norelco" x-ray diffraction unit type 12215/0 (Philips Electronic Instruments) shown in Figure 2 was used and experiments were conducted with x-rays produced at 10 milliamperes and 20 kilovolts.

X-ray diffraction curves were obtained at two "peaks" for each sample, before and after exposure. For zinc samples peaks chosen were at 82.05° and 116.35°; however, for galvanized steel peaks had to be located for each sample by scanning through the entire range of angles. Mounting position was marked on each sample to eliminate errors in the post-exposure measurements due to sample location on the sample holder. Using an angle scanning speed of 0.25° per minute, a plot containing the peak was obtained on a pre-calibrated chart of a millivolt recorder.

RESULTS AND DISCUSSION

A visual examination of the corrosion films formed on the samples showed that the films produced from exposure to the atmosphere were uniformly spread over the entire surface area, greyish in color and free of localized pitting. There was a marked change in the appearance of the shiny surface of clean samples even after a three-day exposure. The films produced in the spray cabinet, on the other hand, were whitish-grey in appearance, spongy in texture and less uniform (Figure 7). Films on samples exposed for a short duration (up to one day) were discontinuous. In fact they consisted of very small dots scattered uniformly over the surface. This observation is not unexpected in view of the manner in which corrosion of samples takes place in the spray cabinet. Fine drops of spray (water) settle on the test surface and react with the adjacent metal in the presence of the oxygen in the air. Therefore at the initial stages the corrosion pattern is drop-wise. As time passes the number of drop-wise corrosion cells increases until 100% of the surface is covered and results in a continuous film. Samples exposed in the spray cabinet for one day or more had continuous films.

Metallographic examination of the corroded samples in general agreed with visual observations. However, at

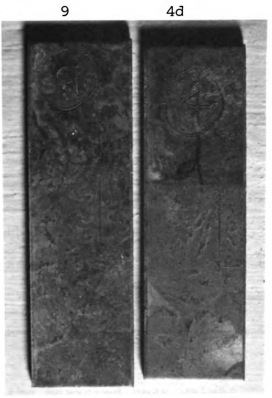

Galvanized steel.
Atmospheric test.

Galvanized steel.
Cabinet test.

Zinc. Atmospheric test.

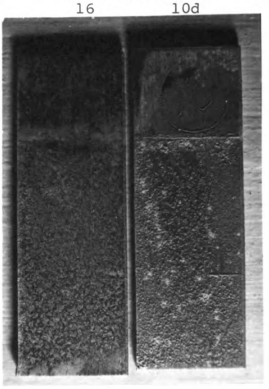

Zinc. Cabinet test.

Figure 7. Corrosion films on some representative samples of zinc and galvanized steel. See Table 1 for exposure times for sample numbers marked.

high magnification (400 x) shiny metal background was seen in spots for all but the 3-week and 4-week exposure samples from the cabinet test.

Measurement of Film Thickness

The x-ray diffraction method failed to measure the thickness of the corrosion films both on zinc and galvanized steel samples. According to the equation $I = I_o e^{(-\frac{\mu}{\rho})\rho x}$ the diffraction peak values of corroded samples were expected to be smaller than the values for the corresponding clean samples as outlined in the previous chapter. However, the measured peak values for corroded samples were inconsistent and in some cases were even higher than the clean samples. Whereas the inconsistent behavior could be explained as due to the uncontrolled variations in the structure (grain size, orientation, etc.) and irregularities of the corroded surface, the higher peak values after corrosion could be possible only if the values measured on clean surfaces were erroneously too low. To investigate the variations in repeated measurements of peak values of diffraction from a clean surface, a new set of samples consisting of four zinc and four galvanized steel samples was prepared. Each sample was mounted on the sample post of the x-ray machine at a fixed (peak) angle determined previously. The diffraction peak values were measured (on both the recorder chart and the counter) three times without changing the sample position or the x-ray settings. The variations

among the repeated measurements ranged from a minimum of 20% to a maximum of 45%. Such large variations (which evidently caused the error in the data) in measurements from the same sample without any change, deliberate or otherwise in any of the influencing factors could not be explained. Under these circumstances the feasibility of this method for corrosion film measurements was not pursued any further.

Film thickness values obtained by metallographic method and by weight-change method (on removal of corrosion products) are tabulated in Table 1.

A comparison of the values measured by the two methods showed that the values given by the metallographic method were in general smaller than those given by the weight-change method. The difference was more pronounced for cabinet test samples where the metallographic values were lower by a maximum amount of 18%. For the atmospheric test samples the difference was small and the metallographic values were lower by a maximum of about 8%.

The difference in film thickness values obtained by the two methods can be explained from the consideration of the following:

1. The weight-change method gives an average value for the film on the entire surface of the test sample. But the metallographic method measures the average film thickness only at the cross-section viewed in the metallograph (Figure 9). These values will

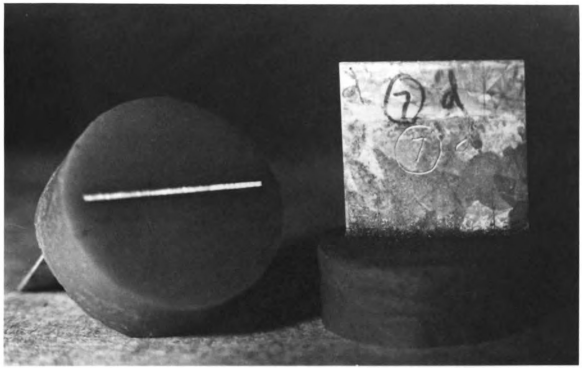

Figure 8. A close-up of the test samples imbedded in 1" diameter plastic mold.

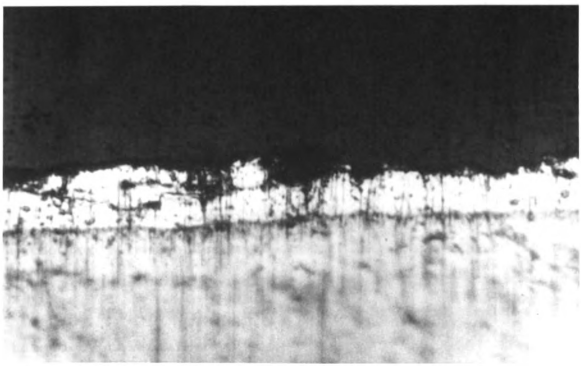

Figure 9. A micrograph of the surface corrosion film (1000 magnification). The dark area is the plastic, the intermediate band is the corrosion film and the light area is the zinc substrate.

therefore vary with the choice of the surface viewed. For relatively uniform films the effect due to the choice of location will be small and hence the metallographic measurements will differ only slightly from the average values measured by the weight-change method. However, for relatively rough films like those on the cabinet-test samples, the choice of the location becomes more important and large variations among the two methods can be expected.

2. In the metallographic method some of the film material may be lost during the polishing operations resulting in measured film values smaller than the actual. The amount of the loss will depend, among other things, on the nature and the characteristics of the film. A rough and less adherent film, as on cabinet-test samples, is more susceptible to mechanical damage than the relatively smooth and adherent films produced on the atmospheric-test samples.

Therefore it can be concluded that the metallographic method of film measurements in the form investigated in this study is applicable to adherent films of uniform thickness. For adherent films of non-uniform thickness the values obtained by this method must be interpreted as the "local" rather than the "average" film thicknesses.

For non-adherent (loose) films special preparations are required to prevent mechanical damage to the film during polishing. In this investigation cold plastic mold was used (Figure 8) for this purpose which did not prove completely satisfactory. Electroplating the film before imbedding the sample in the plastic mold could perhaps be tried to advantage.

Rate of Growth of Corrosion Films

Thickness of corrosion films produced on zinc and galvanized steel samples exposed for different durations to the spray cabinet and the outside atmosphere are shown in Table 1. Also the graphs of film thickness build-up with time are plotted in Figure 11 for the spray cabinet and in Figure 10 for the external atmosphere.

Figure 10 shows that for zinc the rate of film growth is large during the first 2 weeks and then tapers off to a slow rate. The decrease in the growth is more gradual for galvanized steel samples which also show large rates at the beginning. Therefore at the end of the 12-week exposure period (in the atmosphere) zinc samples had already formed protective layers on the surface; however, the galvanized steel samples were still undergoing corrosion at a sizeable rate.

In the cabinet test, on the other hand, both the zinc and the galvanized steel samples corroded at the same rate as shown in Figure 11. Once again the film growth

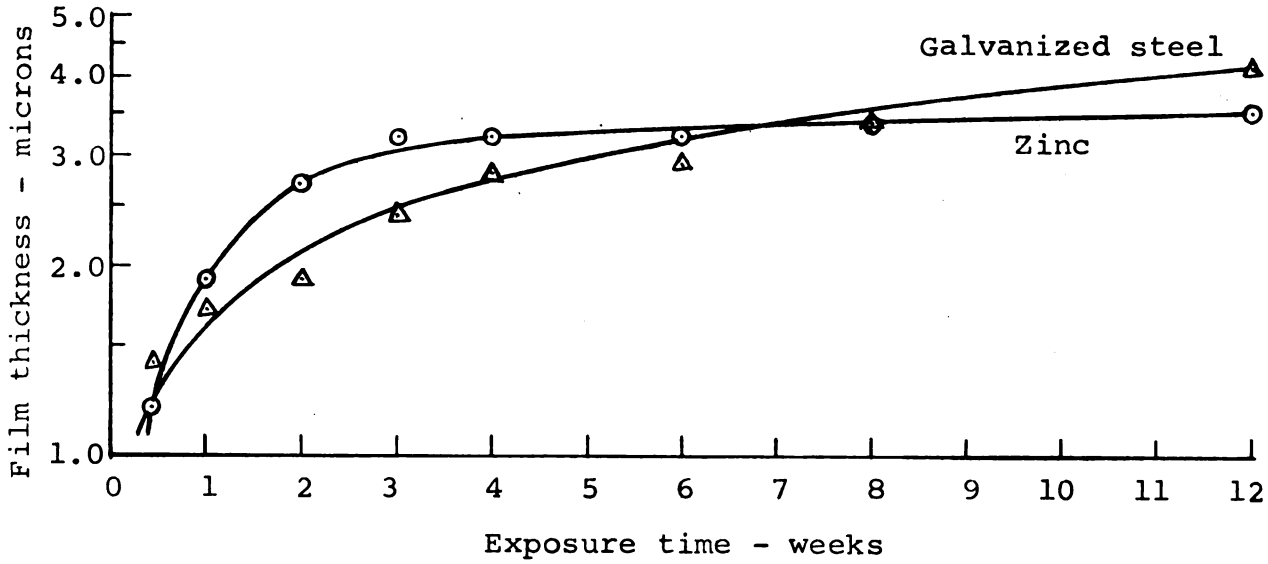

Figure 10. Oxide layer development on zinc and galvanized steel exposed to the atmosphere.

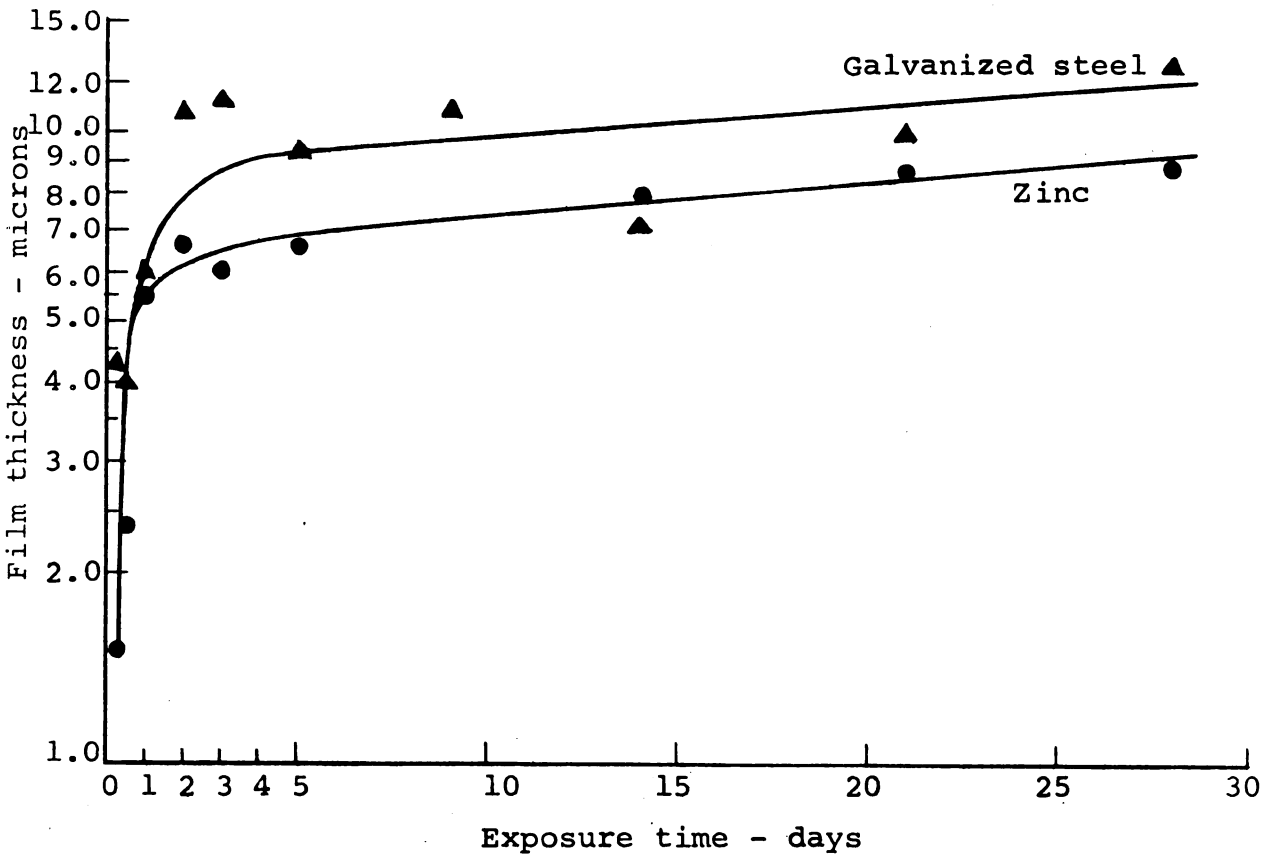

Figure 11. Oxide layer development on zinc and galvanized steel exposed in the spray cabinet.

rate was very large in the first 2 days, then sharply dropped off to a moderate rate for the rest of the exposure time.

In both the atmospheric test and the cabinet test the corrosion films on zinc and galvanized steel samples were of the same order of magnitude. The galvanized steel films were large in absolute value for all but the short duration samples of the atmospheric test as seen in Figures 10 and 11.

For reasons discussed in Chapter 3, no attempt was made to correlate the results of the cabinet test with those of the atmospheric test.

Surface Roughness Measurements

The root mean square (r.m.s.) roughness values of clean metal surfaces, corroded (oxidized) surfaces and the metal surfaces after removal of the oxides as measured by a Micrometrical Profilometer (type "QA") are presented in Table 2. The values shown are the average values for the respective surfaces.

As seen from this table, the variations in the surface roughness of the clean samples of zinc and galvanized steel were small and the absolute values ranged between 0.12 and 0.15 microns for zinc and between 0.25 and 0.30 microns for galvanized steel. However, for corroded surfaces the variations were large, especially on cabinet-test samples. The values ranged between 0.20 - 0.56 microns for zinc and 0.36 - 0.89 microns for galvanized steel in

the atmospheric test and between 0.41 - 2.54 microns for zinc and 0.58 - 4.45 microns for galvanized steel in the cabinet test. The corresponding values after removal of the corrosion products from the sample surfaces were small. This should be expected from the fact that the densities of zinc and zinc oxide differ roughly by a factor of 1-1/2 : 1. Therefore for the same surface area a unit volume of zinc will produce, on corrosion, about 1-1/2 units of zinc oxide which will cause larger irregularities on the surface.

Hemispherical Reflectance Measurements

The hemispherical reflectance, by definition, is the ratio of the total amount of energy reflected in all directions in space to the energy incident from a specified direction (normal in this case) The spectral hemispherical reflectance then refers to the hemispherical reflectance when a monochromatic wave is used.

The graphs of hemispherical reflectance for clean samples of zinc and galvanized steel in the wavelength range 0.35 to 2.75 microns are presented in Figure 12. The values used in these graphs were averaged over all the samples. An infrared absorption peak is observed at 1.0 micron which agrees with the observations of Bor et al (1939) and Coblentz (1920).

The curves for zinc and galvanized steel are almost identical, the galvanized steel curves being lower by an amount 0.08 - 0.10 throughout.

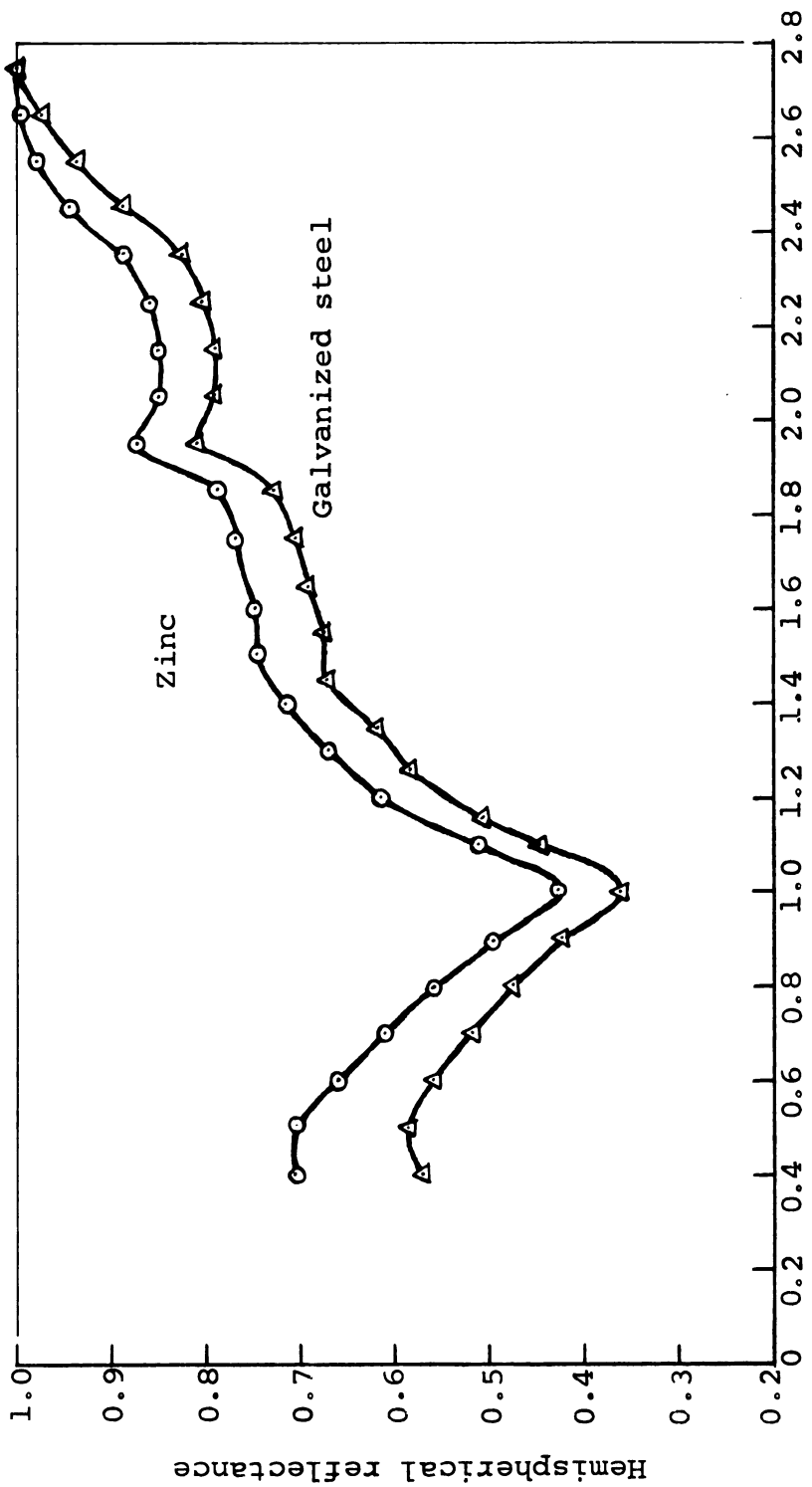

Figure 12. Spectral hemispherical reflectance of clean zinc and galvanized steel in the wavelength range 0.40 to 2.75 microns.

The hemispherical reflectance curves for corroded samples of zinc and galvanized steel were obtained in the same manner as for the clean samples (using Beckman DK-1A Spectrophotometer). The characteristic absorption peak at 1.0 micron was observed in every case. The shape of these curves was essentially similar to that of the clean samples. Since the change in reflectance due to corrosion rather than actual reflectance was of interest in this study, the reflectance curves of corroded samples are not shown here. Instead, the change in reflectance computed from measurements on clean and corroded surfaces (of the same sample) at 0.1 micron intervals in the wavelength range 0.35 - 2.75 microns are presented in Figures 13, 14, 15 and 16 for some representative samples. The corrosion film thickness and the surface roughness values for the samples are marked on each figure.

From Figures 13 and 14 it is seen that for atmospheric test samples (of both zinc and galvanized steel) the decrease in reflectance was large at short wavelengths then declined gradually with increasing wavelengths. For zinc samples the decrease in the hemispherical reflectance was between 0.28 and 0.37 at 0.35 microns and between 0.0 and 0.04 at 2.75 microns, whereas for galvanized steel samples the values ranged between 0.12 and 0.26 at 0.35 microns and between 0.0 and 0.06 at 2.75 microns wavelength.

For cabinet-test samples, however, the decrease in reflectance was seen to be more constant throughout the range

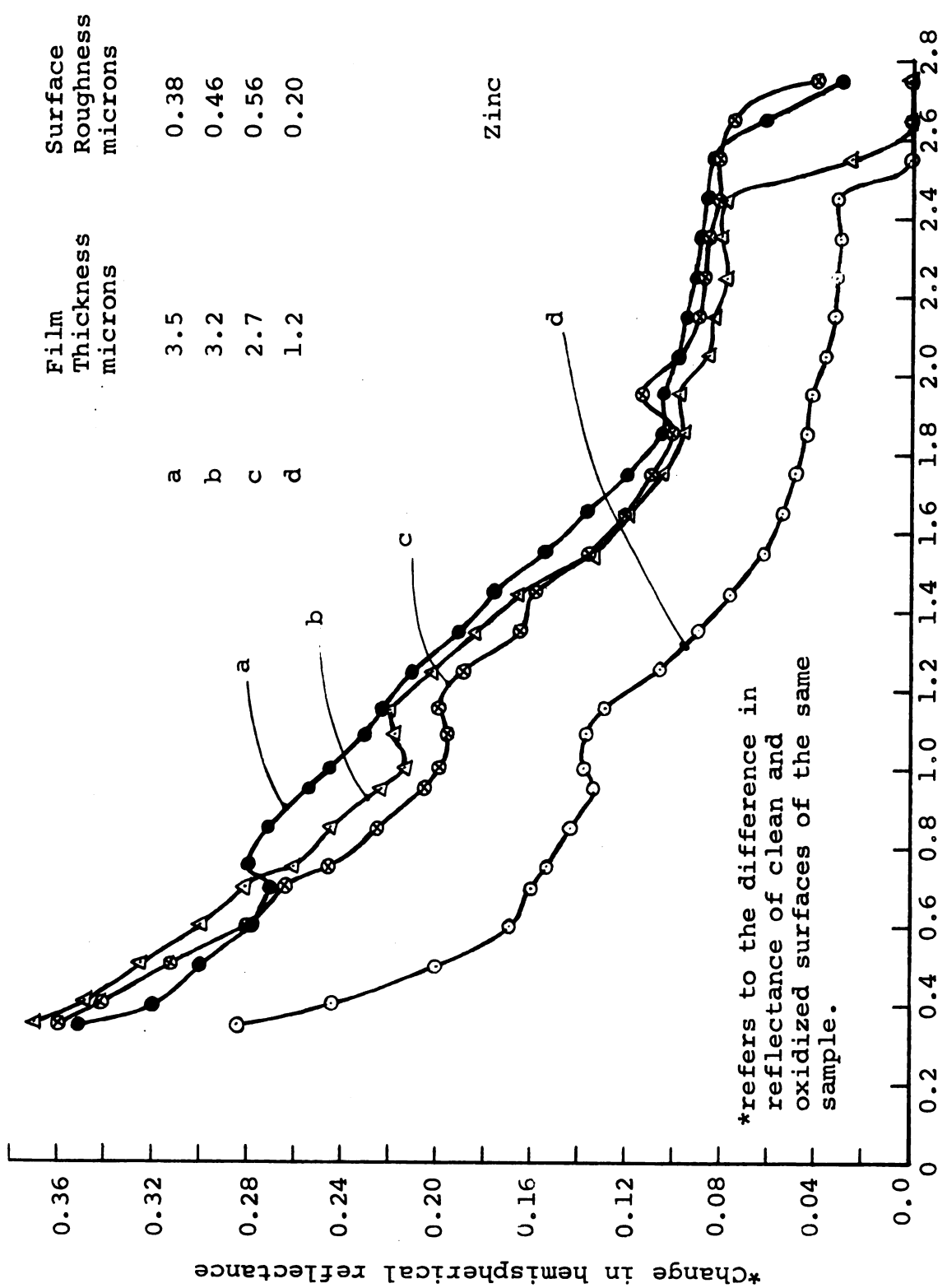

Figure 13. Spectral attenuations of hemispherical reflectance due to oxide layer on zinc exposed to the atmosphere.

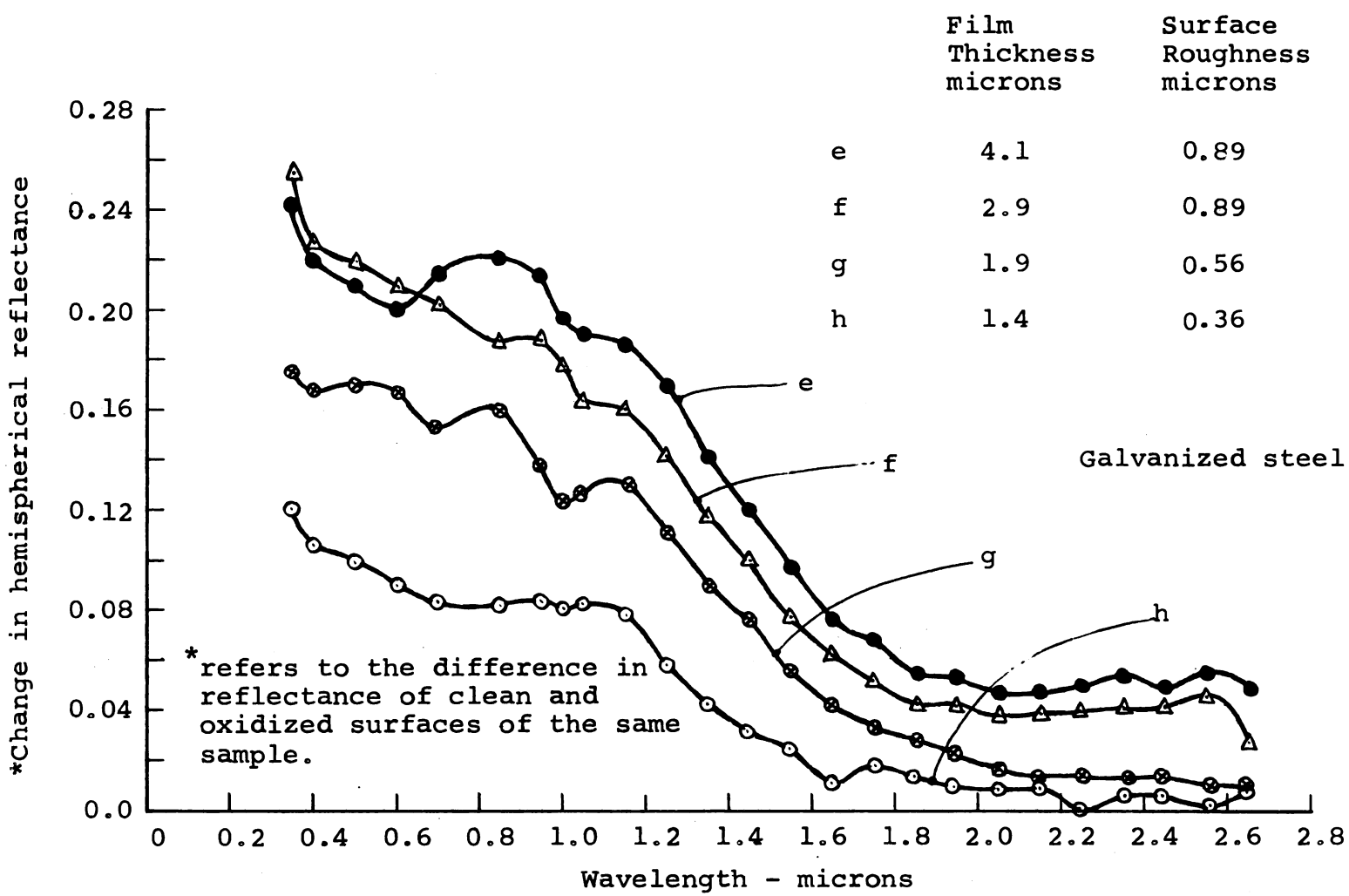

Figure 14. Spectral attenuations of hemispherical reflectance due to oxide layer on galvanized steel exposed to the atmosphere.

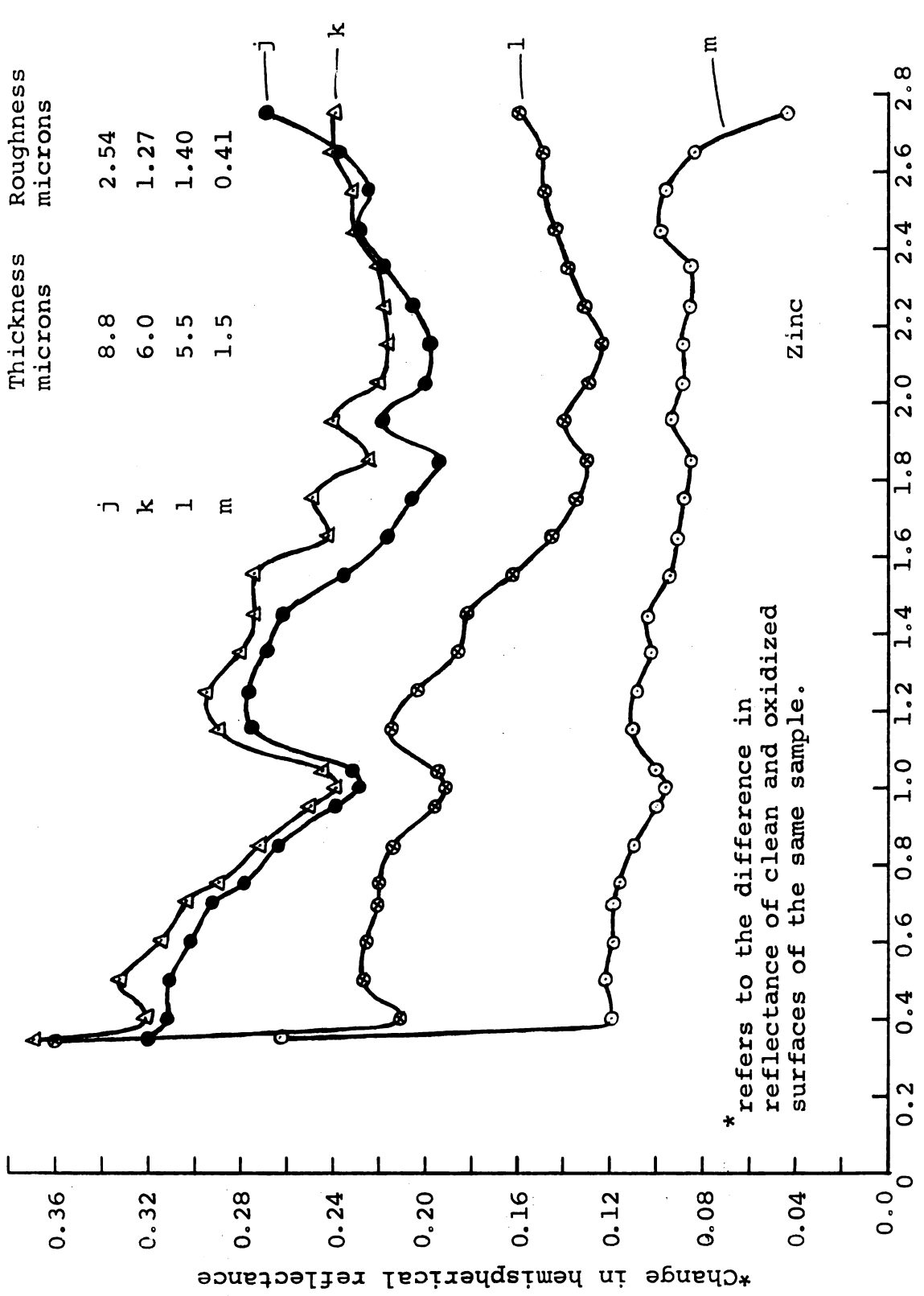

Figure 15. Spectral attenuations of hemispherical reflectance due to oxide layer on zinc exposed in the spray cabinet.

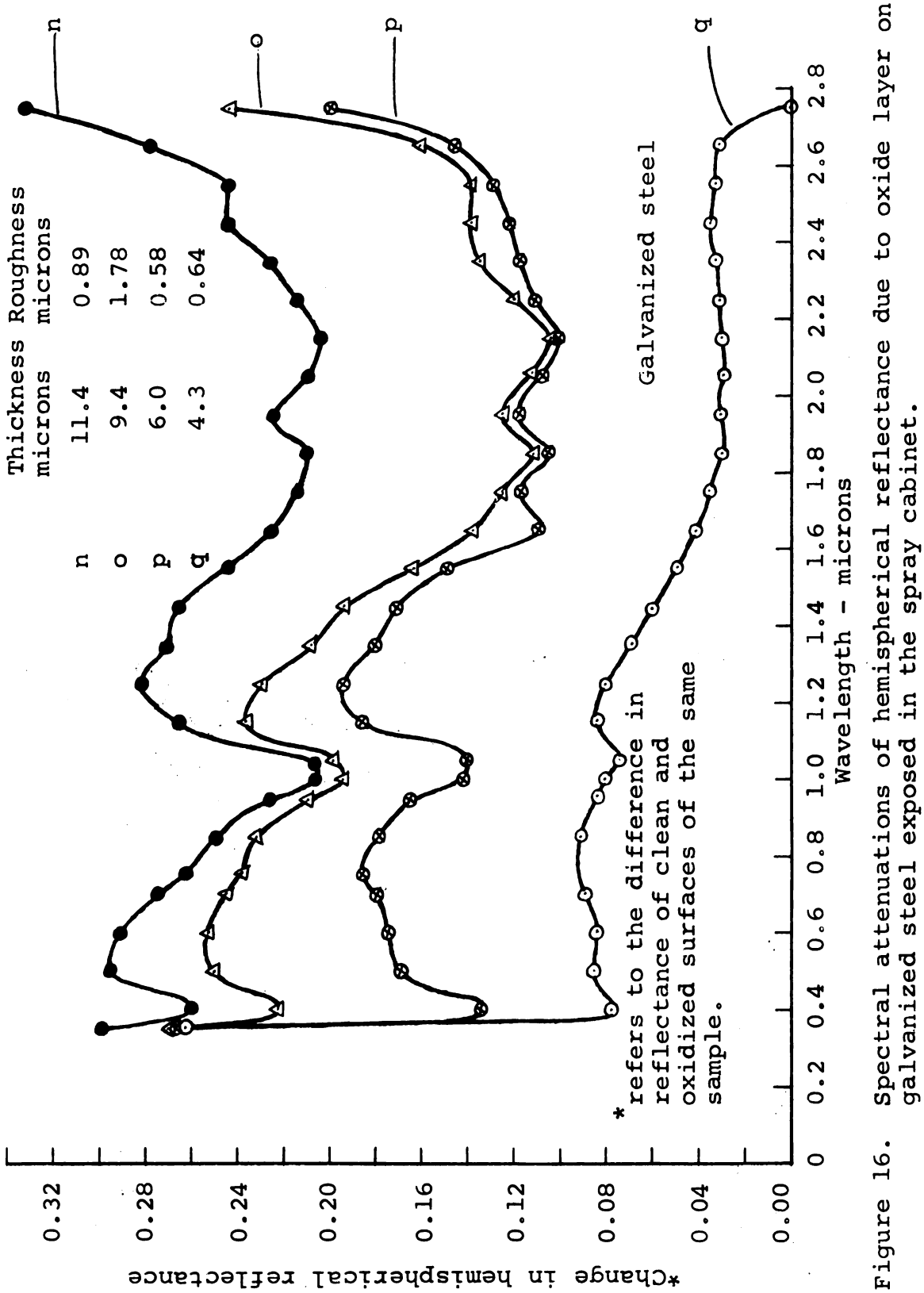

Figure 16. Spectral attenuations of hemispherical reflectance due to oxide layer on galvanized steel exposed in the spray cabinet.

of wavelengths for all but the short exposure samples. For samples exposed for 1 day or more the absolute decrease in reflectance varied between 0.10 and 0.30 in the wavelength range considered except the two extremes where the variations were large.

Mean Integrated Hemispherical Reflectance

The hemispherical reflectance curves discussed thus far were obtained using monochromatic waves of constant intensity. However, the intensities of radiations for the real sources are not uniform but exhibit a definite distribution over the range of wavelengths. Therefore to investigate the optical behavior of a surface exposed to a real source, the hemispherical reflectance curves should be normalized with the energy distribution curves of the source. The average value of the resulting curve (which is used as a criterion of the optical behavior) is called the mean integrated hemispherical reflectance. Mathematically it can be expressed (assuming the source to be a black body or a grey body) as:

$$\text{Mean integrated hemispherical (MIH) reflectance} = \frac{\int R_\lambda \, e_{b\lambda} \, d\lambda}{\int e_{b\lambda} \, d\lambda}$$

where the emissive power $e_{b\lambda}$ is obtained from Planck's expression

$$e_{b\lambda} = \pi i_{bn\lambda} = \frac{2\pi c_1}{\lambda^5 \left(e^{c_2/\lambda T} - 1\right)}$$

c_1 = 0.18892 x 10^8 BTU μ^4/hr ft^2 (Planck's constant)

c_2 = 25,896 $\mu^{\circ}R$ (Stefan-Boltzman constant)

T = source temperature, $^{\circ}R$

λ = wavelength of radiation, microns

R_λ = spectral hemispherical reflectance

The mean integrated hemispherical (MIH) reflectance values for the samples were calculated (by computer) using $d\lambda$ intervals of 0.05 microns for a 10,000$^{\circ}R$ source (sun) and a 3000$^{\circ}R$ source (tungsten lamp). These values are given in Table 3 and are plotted against exposure time of the samples in Figures 17 and 18.

The graphs of zinc and galvanized steel are seen to be almost identical, particularly after long exposures. These graphs clearly show that the major portion of the change in the optical properties of the corroding samples of zinc and galvanized steel took place in the first three days of exposure in the cabinet and in the first two weeks when exposed to the outside atmosphere. The changes at subsequent times were small. For a 10,000$^{\circ}R$ source (sun) the integrated total reflectance values for zinc decreased from 0.64 (for clean samples) to 0.35 in the cabinet and to 0.37 in the external atmosphere, and from 0.55 to 0.33 and 0.35 respectively for galvanized steel samples. Similarly, for the 3000$^{\circ}R$ source the values decreased from 0.80 to 0.55

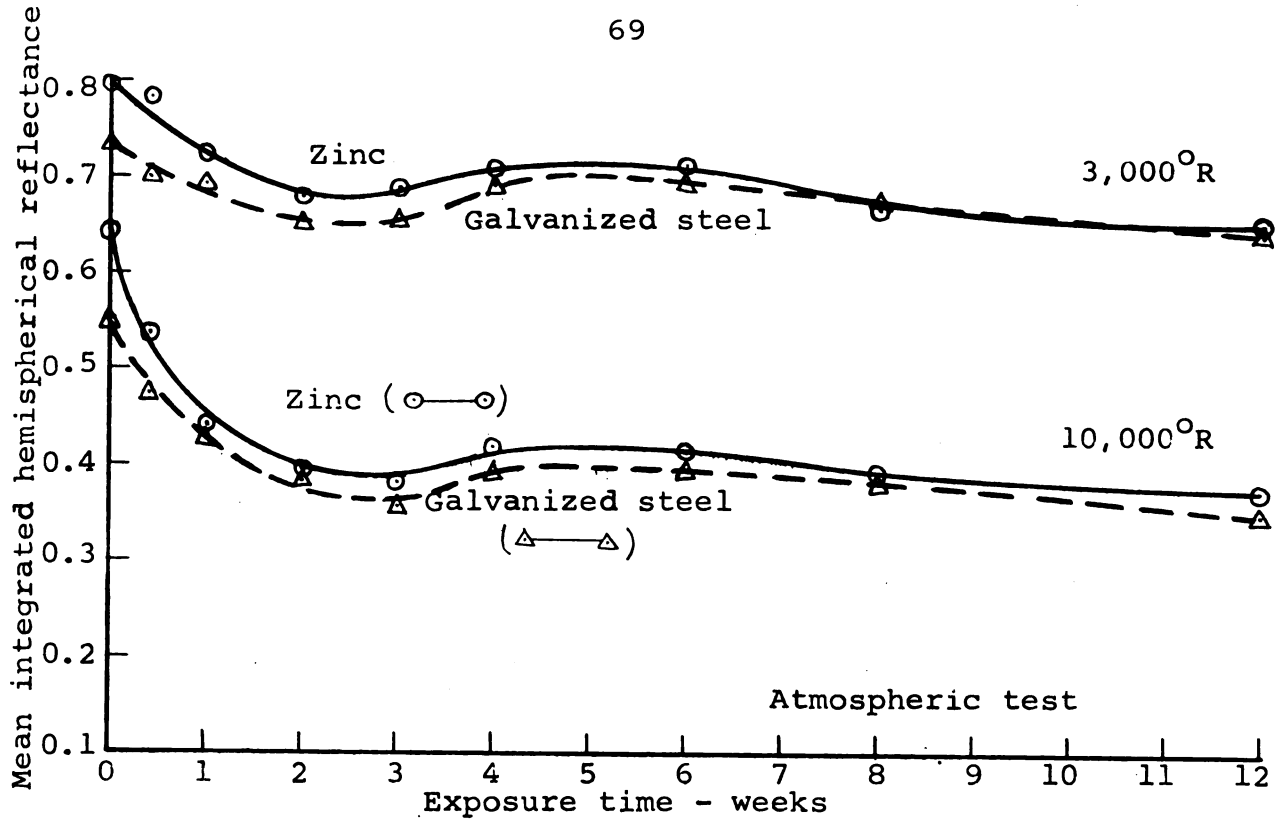

Figure 17. Change in the mean integrated hemispherical reflectance of zinc and galvanized steel versus time of exposure to the atmosphere.

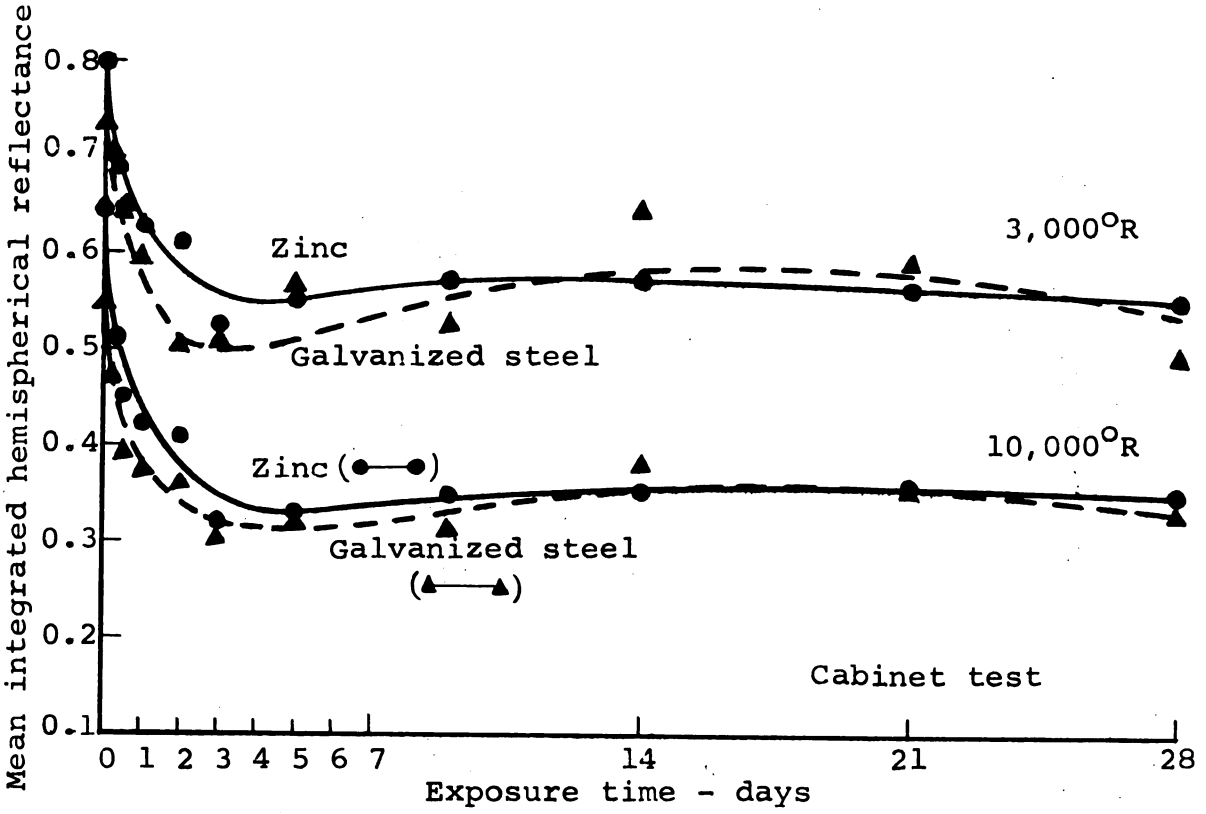

Figure 18. Change in the mean integrated hemispherical reflectance of zinc and galvanized steel versus time of exposure in the spray cabinet.

and 0.65 for zinc and from 0.73 to 0.54 and 0.64 respectively for galvanized steel.

Therefore the increase in the total integrated absorptance (complement of reflectance) due to corrosion was 75-80% for zinc and 45-50% for galvanized steel for radiations from a 10,000^{o}R source. For 3,000^{o}R source, on the other hand, the increase was 75 to 125% for zinc and 33 to 70% for galvanized steel.

Effect of Corrosion Film Thickness on the Mean Integrated Hemispherical Reflectance

Experimental results: The experimental values of the MIH reflectance of clean and corroded samples (from Table 3) are presented graphically in Figure 19 as a function of the corrosion film thickness of zinc and galvanized steel samples (combined). Figure 19 shows that for the 10,000^{o}R source nearly 75% of the total decrease in the MIH reflectance occurred in films 3.0 microns thick. However, for the 3000^{o}R source the decrease in MIH reflectance was almost constant throughout. The mean integrated hemispherical absorptance increased by 76% for 10,000^{o}R source and by 117% for 3000^{o}R source.

Theoretical results: In Chapter 3, theoretical equations were derived based on the Maxwell's theory of wave propagation through stratified media to predict the behavior of hemispherical reflectance from smooth surfaces as a function of the film thickness. These equations consider the changes due only to multiple reflections within the film

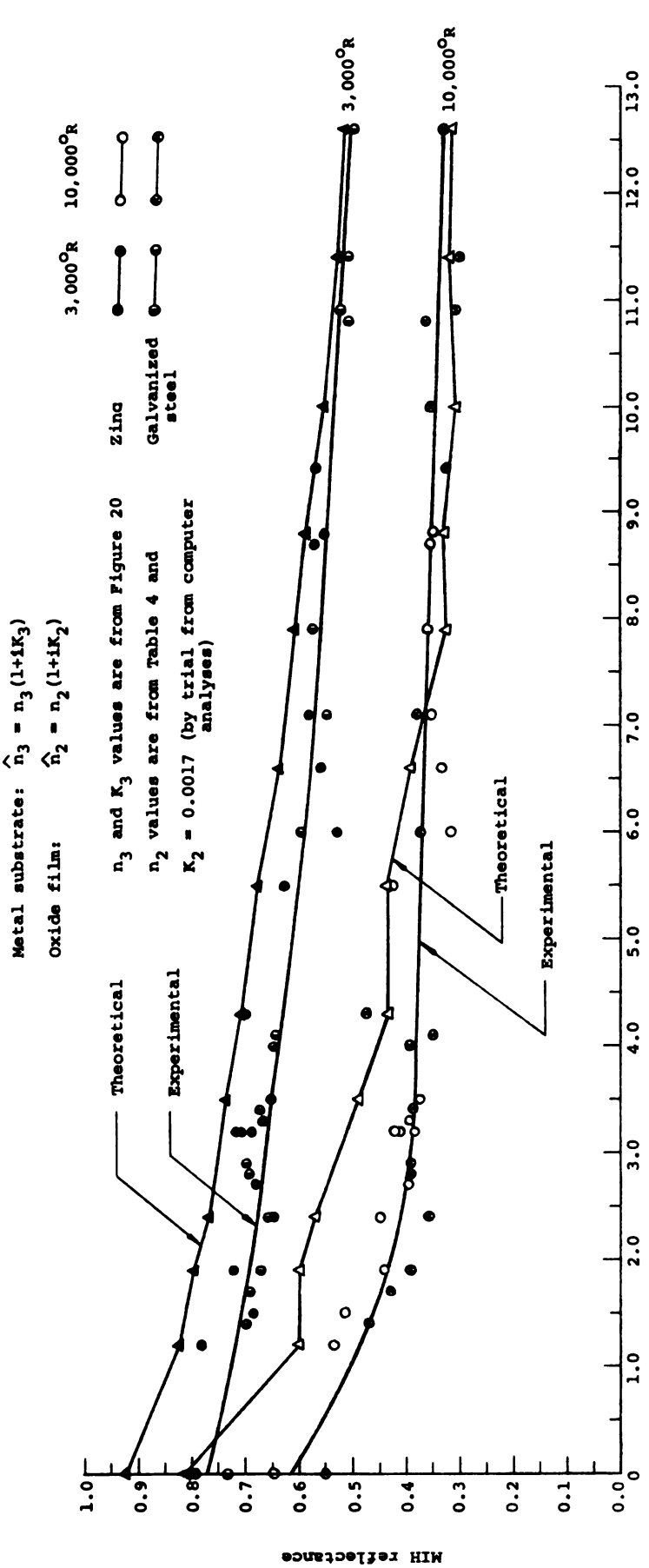

Figure 19. Mean integrated hemispherical reflectance versus oxide film thickness.

which is assumed to have smooth surfaces. Therefore the effect of the surface roughness is ignored.

In order to obtain the behavior curves from these equations it is necessary to know the spectral values of the optical constants n (refractive index) and K (the extinction coefficient) of the film material and the substrate metal. A search through the literature revealed that such information is not available for bulk materials except in the visible range. The spectral values of optical constants of thin evaporated films measured by polarimetric methods have been reported. However, these values may differ greatly from those of the bulk material (Scott, 1955) and hence are not reliable. Therefore it was decided to extrapolate the known bulk values to the long wavelength region using valid approximations.

The reported values (International Critical Tables, 1929) of the refractive index and the extinction coefficient of zinc and the refractive index of ZnO are shown in Table 4. The refractive index values of ZnO become very nearly constant beyond 0.7 microns. Therefore a constant value of 1.96 was used for longer wavelengths. The n and K values of zinc are plotted in Figure 20. The refractive index curve was extrapolated to follow the Hagen-Rubens approximation which is valid strictly in the long wavelength region (Born, 1964, p. 622). The extrapolation of the extinction coefficient curve was based on the assumption that when n is large ($n \gg 1$) then K approaches 1 (Born, 1964, p. 615).

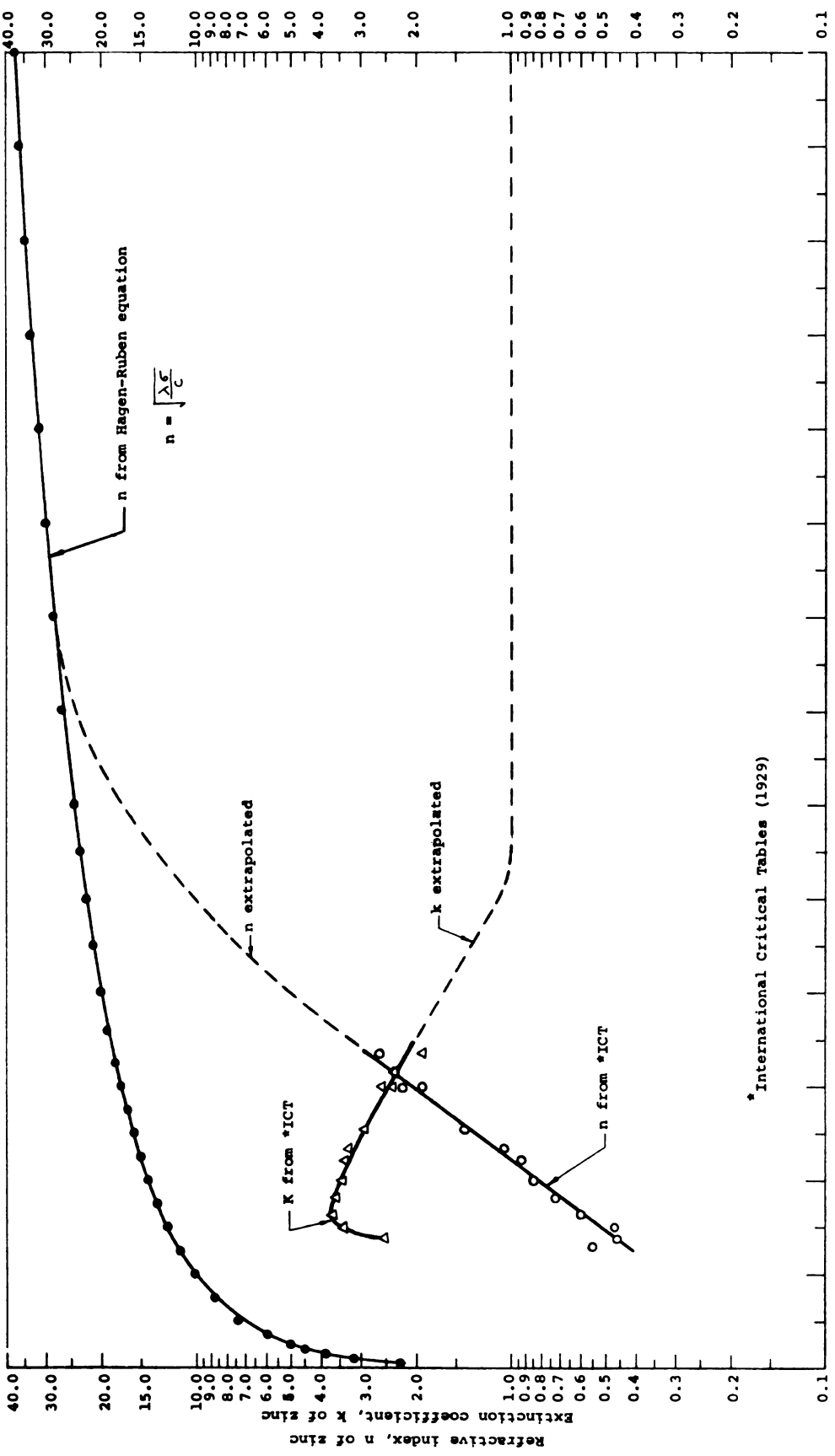

Figure 20. Extrapolation of refractive index (n) and extinction coefficient (k) values of zinc.

Such approximations are bound to introduce errors in the analysis but more exact data are not available.

Equations (40), (53) and (57) in Chapter 3 give the reflectance behavior of a dielectric film in the air, a dielectric film over a metallic substrate (in air) and an absorbing film over a metallic substrate (in air) respectively. By substituting the spectral values of n and k in these equations the reflectance curves for the range of film thicknesses can be obtained. The corresponding integrated reflectance curves can then be computed by the process outlined earlier in this Chapter.

The zinc oxide-zinc composite media formed by the corrosion of zinc will fit in one of the last two models above depending on whether the extinction coefficient K_2 of the ZnO film is equal to zero or has finite value greater than zero.

In Figures 21 and 22 the mean integrated hemispherical reflectance curves for this composite media (calculated from equations 53 and 57) are presented for K_2 values ranging from 0.0 - 0.857. It is interesting to observe that the mean integrated reflectance values at first decreased with increase of K_2 values from 0.0 - 0.10 and then increased as K_2 increased from 0.1 - 0.857. This may be explained as follows:

When K_2 = 0.0, 100% of the refracted wave traveling through the film reaches the metal which, being a good reflector, reflects most of it back. Hence the reflectance is high. As K_2 increases, more and more of the refracted

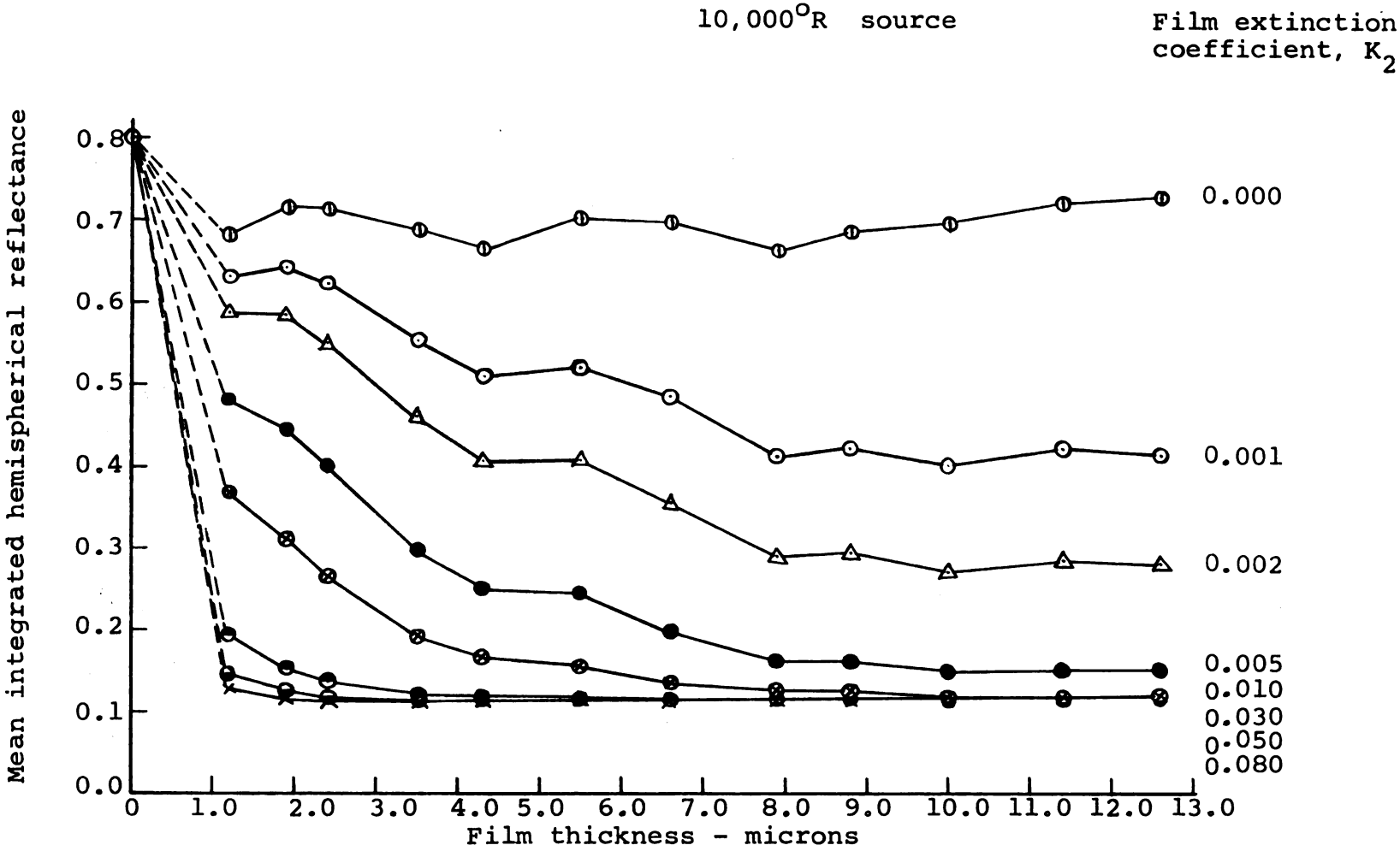

Figure 21. Effect of the film extinction coefficient (in the range 0 to 0.08) on the theoretical MIH reflectance of the film-metal composite. Source temperature: 10,000°R.

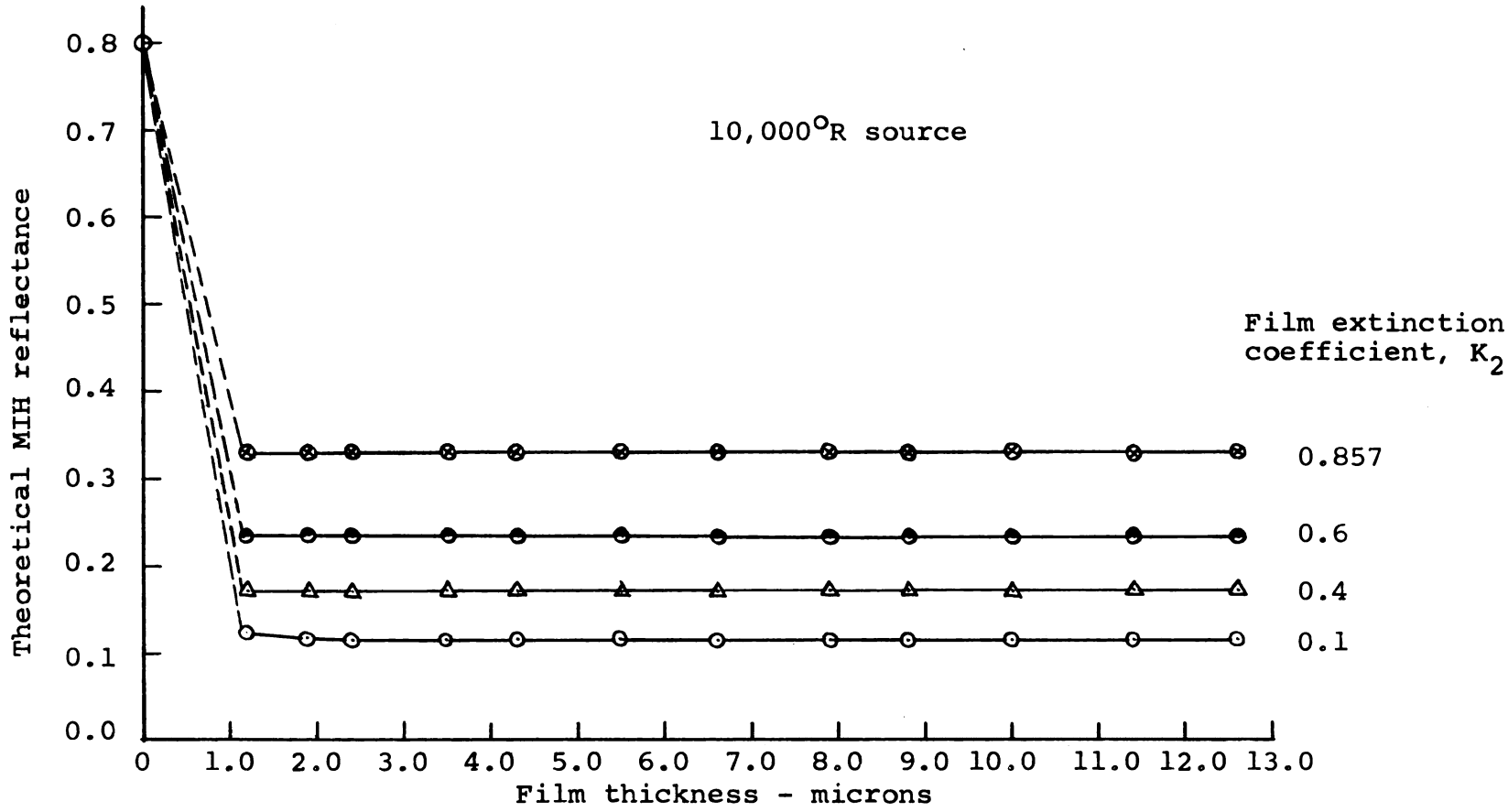

Figure 22. Effect of the film extinction coefficient (in the range 0.1 to 0.857) on the theoretical MIH reflectance of the film-metal composite. Source temperature: 10,000°R.

wave is attenuated during its passage through the film and therefore less of it strikes and is reflected back from the metal surface. Therefore the reflectance decreases. Eventually a value of K_2 is reached when all of the refracted wave is absorbed in the film and none reaches the back metal. The contribution of the metal (substrate) becomes zero. The film then acts as a thick absorbing film in the air and the reflection behavior is determined entirely by the properties of the film. Since the multiple reflections within the film are then nonexistent, the effect of the film thickness, too, becomes negligible. As K_2 increases further, the reflectance increases since the wave which is absorbed in a thin layer of the film next to the interface is bounced back (Wolf, 1964, p. 615).

The integrated total reflectance curves calculated with $K_2 = 0.0017$ showed closest agreement with the experimental data. Figure 19 shows that whereas the agreement was good for thick films, large discrepancies existed for films of small thicknesses. This can be explained from the fact that for thick films the effect of multiple reflections within the film is predominant and the error from neglecting surface roughness is small. For relatively thin films, however, the effect of surface roughness is large and therefore large errors result if this effect is not accounted for in the analysis.

To investigate the influence of surface roughness on the integrated hemispherical reflectance of zinc and

galvanized steel samples, the reflectance data was plotted against the r.m.s. roughness values of the corrosion film. As seen from Figures 23 and 24, the data showed a tendency toward a smooth curve for both 3000°R and 10,000°R sources. This suggested, at least qualitatively, that correlation did exist between the two factors. The trends of these curves were in general agreement with those reported by Birkebak et al (1964) even though the two situations were quite different as discussed in the Review of Literature.

Since the variations of the surface roughness of the corrosion film as well as the underlying metal were uncontrolled and the geometrical shape of the irregularities was not known, no attempt was made to draw any quantitative conclusions. It is left to the future researchers working with controlled films of known surface conditions to study (quantitatively) the relative effects of the surface films due to the multiple reflections, and from the surface roughness due to systematic scattering depending on the shape of the irregularities.

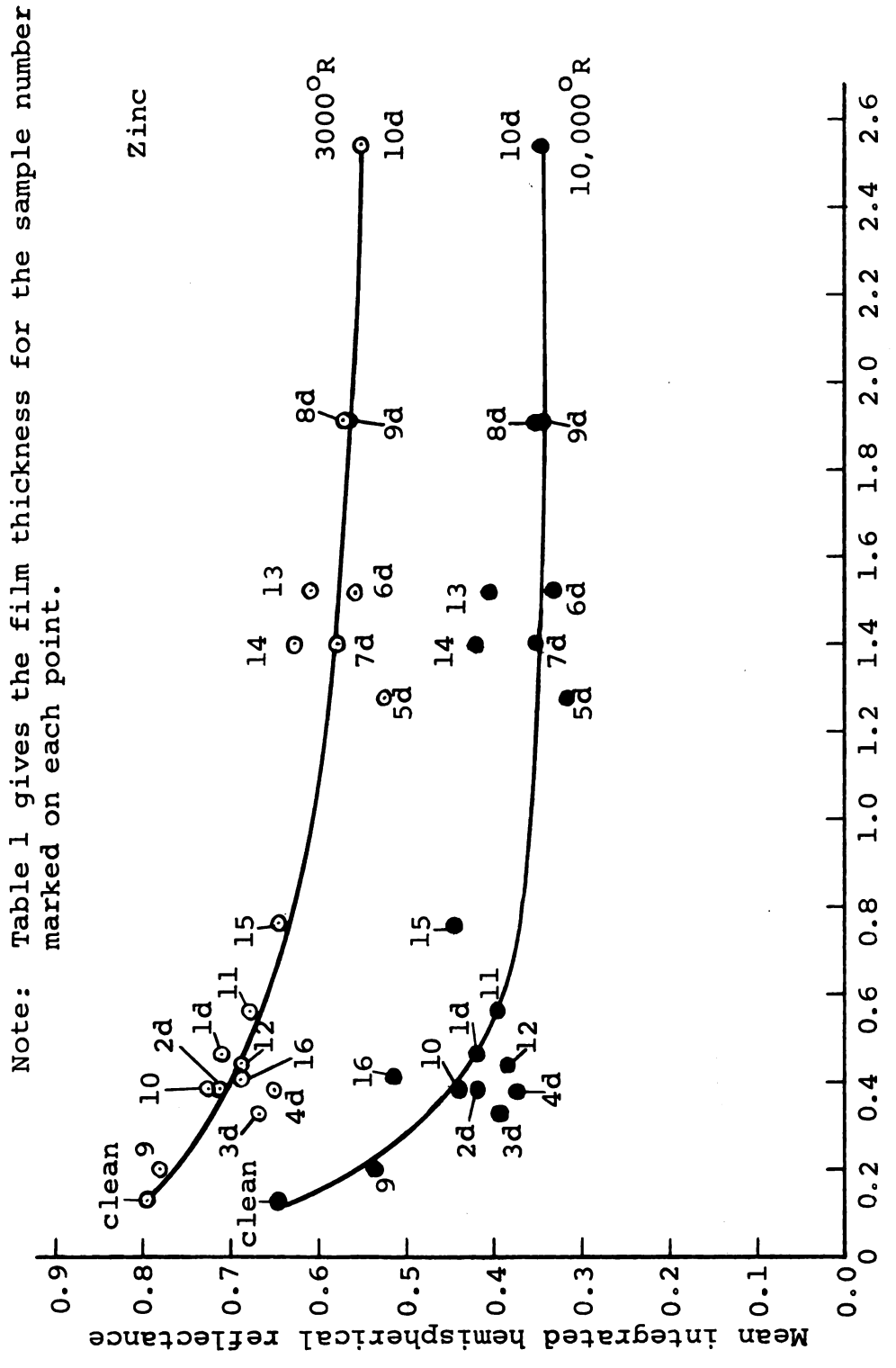

Figure 23. Correlation of the MIH reflectance with the surface roughness of the oxide films on zinc samples.

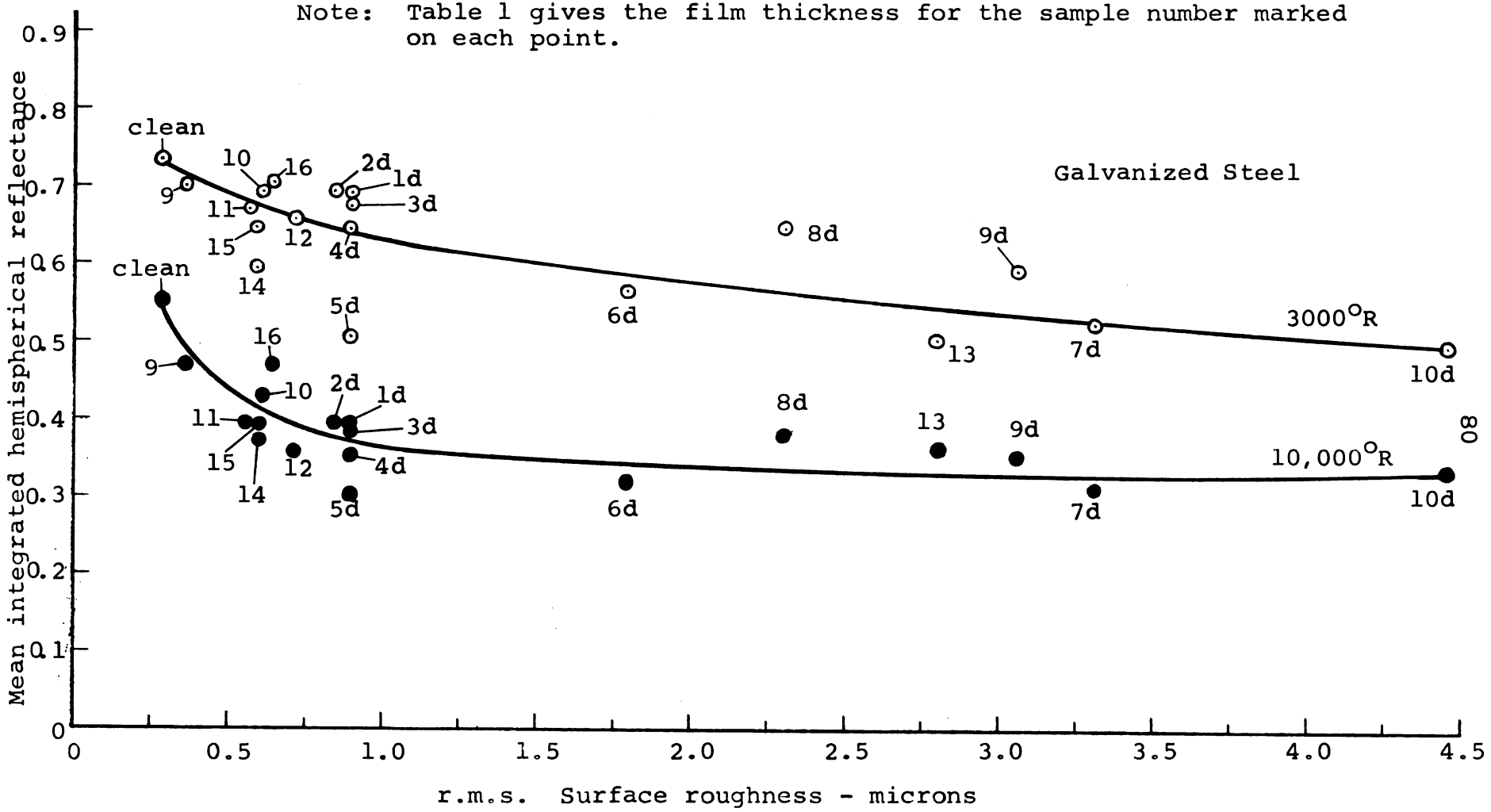

Figure 24. Correlation of the MIH reflectance with the surface roughness of the oxide films on galvanized steel samples.

SUMMARY

The purpose of this study was to determine the corrosion rates of zinc and galvanized steel and to relate their optical properties to the amount of corrosion in the radiation spectrum of 0.35 to 2.75 micron wavelengths from a 10,000°R source (sun) and a 3000°R source (tungsten lamp).

Samples of zinc and galvanized steel were corroded for several durations up to 3 months in outdoor atmosphere and up to 4 weeks in a spray cabinet using a continuous spray of water. The corrosion film thicknesses were measured by the weight-change method (removal of the corrosion products from the test surface), by the x-ray diffraction method and by the metallographic method.

A Beckman DK-1A ratio recording spectrophotometer with a Beckman 24500 reflectance attachment was used to measure the hemispherical reflectance at normal incidence in the wavelength range 0.35 to 2.75 microns. The hemispherical reflectance curves so obtained were normalized with the energy distribution curves of the 10,000°R and the 3000°R sources to obtain the corresponding integrated hemispherical reflectance curves. The average of these curves, called mean integrated hemispherical (MIH) reflectance, were used as a criterion for the optical behavior of the samples.

The corrosion films produced in the atmosphere were smoother than those produced in the spray cabinet. The

film thicknesses varied from 1.2 to 12.6 microns. The rate of corrosion was appreciable for the first 2 weeks in the atmosphere and the first two days in the spray cabinet. In the remaining period the rate was relatively small.

The MIH reflectance decreased with the growth of the corrosion films. For the 10,000°R source nearly 75% of the reduction occurred in films 3.0 microns thick, but for 3000°R source the rate was relatively constant at all thicknesses. The corresponding increase in MIH absorptance was 76% for the 10,000°R source and 117% for the 3000°R source.

The experimental values of MIH reflectance were correlated with the theoretical predictions based on the Maxwell's theory of wave propagation through stratified media (assumed perfectly smooth) using a value of 0.0017 for the extinction coefficient of zinc oxide corrosion film. The agreement was good at large film thicknesses but was poor for films less than 4.0 microns thickness. This was attributed to the fact that the effect of surface roughness, which was neglected in the theoretical analysis, was in fact proportionately large at small film thicknesses.

The MIH reflectance showed at least a qualitative correlation with the surface roughness. The trends of the curves were comparable with those reported in the literature. The separate effects of the film thickness and the surface roughness, however, could not be ascertained in this study because of the simultaneous and uncontrolled variations of these factors.

CONCLUSIONS

1. The corrosion films produced in the atmosphere for exposures up to 12 weeks were relatively smooth and were found to vary from 1.2 to 3.5 microns for zinc and from 1.4 to 4.1 microns for galvanized steel. The spray cabinet films ranged from 1.5 to 8.8 microns for zinc and from 4.0 to 12.6 microns for galvanized steel for exposures up to 4 weeks.
2. The rate of corrosion of both zinc and galvanized steel was substantial in the first 2 weeks (of exposure) in the atmosphere and the first 2 days in the spray cabinet. The rate then stabilized to a constant low value.
3. The spectral attenuations in the hemispherical reflectance due to corrosion were seen to vary, depending upon the film thickness, from 0.27 to 0.37 at 0.35 microns and from 0 to 0.04 at 2.75 microns for atmospheric test samples. For cabinet samples, however, the variations were nearly constant throughout the range of wavelengths considered except at the two extremes. This indicated that relatively high absorption took place in the short wavelength region for the samples oxidized in the atmosphere. The absorption increased at all wavelengths for samples corroded in the cabinet.

4. The mean integrated hemispherical (MIH) reflectance decreased with the growth of the corrosion film thickness. For a 3000°R source the reduction in the MIH reflectance was nearly linear but for the 10,000°R source almost 75% of the change occurred in films 3.0 microns thick.

5. The mean integrated hemispherical absorptance (complement of reflectance) of zinc and galvanized steel samples increased by 76% for solar radiations(10,000°R source). For 3000°R source, on the other hand, the increase was about 117%.

6. The theoretical predictions of MIH reflectance based on the Maxwell's theory of wave propagation through stratified media showed best fit with the experimental data using a value of 0.0017 for the extinction coefficient of the zinc oxide corrosion film. The agreement was good for thick films but large discrepancies existed for films below 4.0 microns. This was probably due to the failure of the theoretical analysis to account for the effect of surface roughness which is large for thin films.

7. The MIH reflectance data showed a qualitative correlation with the measured surface roughness values of corrosion films. The trends were comparable with those reported by Birkebak et al (1964). However, no quantitative conclusions were drawn because of the uncontrolled variations of surface

roughness with film growth and unknown geometrical shape of the irregularities.

REFERENCES

REFERENCES

AGNEW, J. T. and R. B. McQUISTAN
1953 "Experiments concerning infrared diffuse reflectance standards in the range 0.8 to 20.0 microns," Journal of Optical Society of America, V 43, n 11, pp. 999-1007.

ANDERSON, E. A.
1946 "The corrosion of zinc in the outdoor atmosphere," symposium on Atmospheric Exposure Tests on Non-Ferrous Metals, Proceedings of the American Society for Testing Materials, pp. 2-14.

AMERICAN SOCIETY FOR TESTING MATERIALS, STANDARDS
1952 "Tentative method of total immersion corrosion test of non-ferrous metals," B 185-43 T. Part II. American Society for Testing Materials. Philadelphia. p. 1327.

AMERICAN SOCIETY FOR TESTING MATERIALS, STANDARDS
1958 "Standard method of total immersion corrosion test for soak tank metal cleaners." D 1280-57. Part X. American Society for Testing Materials, Philadelphia. p. 1498.

AMERICAN SOCIETY FOR TESTING MATERIALS, STANDARDS
1962 "Standard method of salt spray (fog) testing," B 117-62. Part 3. American Society for Testing Materials, pp. 402-409.

BENNETT, H. E. and J. O. PORTEUS
1961 "Relation between surface roughness and specular reflectance at normal incidence," Journal of Optical Society of America, V 51, n 2, pp. 123-129.

BENNETT, H. E.
1963 "Specular reflectance of aluminized ground glass and the height distribution of surface irregularities," Journal of Optical Society of America, V 53, n 12, pp. 1389-1394.

BIRKEBAK, R. C., E. M. SPARROW, E. R. G. ECKERT and J. W. RAMSEY
1964 "Effect of surface roughness on the total hemispherical and specular reflectance of metallic surfaces," Journal of Heat Transfer, V 86, series C, n 2, pp. 193-199.

BIRKEBAK, R. C. and E. R. G. ECKERT
1965 "Effect of roughness of metal surfaces on angular distribution of monochromatic reflected radiation," Journal of Heat Transfer, V 87, series C, n 1, pp. 85-93.

BLUM, W.
1948 "Tests for metal coatings," A paper, pp. 1030-1031, in H. H. UHLIG, ed. The Corrosion Handbook, John Wiley and Sons Inc., New York, 1188 pp.

BOCK, R. O.
1945 "Values of the optical constants for Beryllium, Magnesium and Zinc," Journal of Physical Review, V 68, n 9-10, pp. 210-213.

BORN, M. and E. WOLF
1964 Principles of Optics. Pergamon Press, London. 808 pp.

BRITISH IRON AND STEEL RESEARCH ASSOCIATION
1948 "First report of testing (corrosion) sub-committee," Journal of Iron and Steel Institute, V 158, pp. 463-493.

BUELOW, F. H.
1956 "The effect of various parameters on the design of solar energy air heater," unpublished Ph.D. thesis, Michigan State University, East Lansing, Michigan.

BUELOW, F. H.
1961 "Drying crop with solar heated air," Agenda item III C-3, United Nations Conference on New Sources of Energy.

CAMPBELL, W. E. and U. B. THOMAS
1939 "Tarnish studies. The electrolytic reduction method for the analysis of films on metal surfaces," Transactions of Electrochemical Society, V 76, pp. 303-328.

CHAMPION, F. A.
1952 Corrosion Testing Procedures. John Wiley and Sons, Inc., New York. 355 pp.

CHINMAYANANDAM, T. K.
1919 "On the specular reflection from rough surfaces," Journal of Physical Review, V 13 second series, pp. 96-101.

CLOSE, D. J.
1962 "Flat plate solar absorbers: The production and testing of a selective surface for copper absorber plate," Commonwealth Scientific and Industrial Research Organization. Engineering section report ED 7.

COBLENTZ, W. W.
1920 "Reflection power of monel metal, stellite and zinc," Bureau of Standards, Scientific papers Volume 16, number 379.

CONSTABLE, F. H.
1927 "The cause of the colours shown during the oxidation of metallic copper," Proceedings of the Royal Society, series A, V 115, pp. 570-588.

DANIELS, F.
1955 "Principles and problems in the utilization of solar energy," Conference on solar energy, The scientific basis, at the University of Arizona, Tucson.

DAVIES, H.
1954 "The reflection of electromagnetic waves from a rough surface," Proceedings of the Institute of Electrical Engineers, V 101, pp. 209-213.

DAVIS, C. P. and R. I. LIPPER
1961 "Solar energy utilization for crop drying," Agenda item III C-3, United Nations Conference on New Sources of Energy.

DUFFIE, J. A.
1961 "General report. Agenda title: New materials in solar energy utilization." Agenda item III B. United Nations Conference on New Sources of Energy.

ECKERT, E. R. G. and R. M. DRAKE
1959 Heat and Mass Transfer, McGraw-Hill Book Co., Inc., New York, 530 pp.

EDLIN, F. and D. WILLAUER
1961 "Plastic films for solar energy applications," Agenda item III B. United Nations Conference on New Sources of Energy.

EDWARDS, D., and R. RODDICK
1961 "Spectral and directional thermal radiation characteristics of selective surfaces for solar collectors," Agenda item III B. United Nations Conference on New Sources of Energy.

ELLIS, O. B.
1949 "Effect of weather on the initial corrosion rate of sheet zinc," Proceedings of American Society for Testing Materials, V 49, pp. 152-167.

EUROF, DAVIES D.
1957 "Oxide films on silver at high temperatures," Nature, V 179, n 4573, pp. 1293-1294.

EVANS, U. R.
1961 The Corrosion and Oxidation of Metals. Arnold Publications.

EVANS, U. R. and L. C. BANNISTER
1929 "The growth of silver iodide films," Proceedings of Royal Society, series A, V 125, pp. 370-394.

FRANCIS, J. E. and T. J. LOVE (Jr.)
1966 "Radiant heat transfer analysis of isothermal diathermanous coatings on a conductor," Journal of the American Institute of Aeronautics and Astronautics, V 4, n 4, pp. 643-650.

GORTON, F. A.
1916 "Reflection from and transmission through rough surfaces," Journal of Physical Review, V 7 second series, pp. 66-78.

GWYTHER, R. E.
1947 "Preparation of metals for painting -- a review," Journal of Corrosion, V 3, n 4, pp. 201-207.

HALL, J. F. and W. F. C. FERGUSON
1955 "Optical properties of cadmium sulphide and zinc sulphide from 0.6 micron to 14 microns," Journal of Optical Society of America, V 45, n 9, pp. 714-718.

HARRIS, L., J. K. BEASLEY and A. L. LOEB
1951 "Reflection and transmission of radiation by metal films and the influence of non-absorbing backings," Journal of Optical Society of America, V 41, n 9, pp. 604-614.

HASS, G.
1949 "On the preparation of hard oxide films with precisely controlled thickness on evaporated aluminum mirrors," Journal of Optical Society of America, V 39, pp. 532-540.

HASS, G. and C. D. SALZBERG
1954 "Optical properties of silicon monoxide in the wavelength region from 0.24 to 14.0 μ," Journal of Optical Society of America, V 44, n 3, pp. 181-187.

HEAVENS, O. S.
1965 Optical Properties of Thin Solid Films. Dover Publications, New York.

HILSUM, C.
1954 "Infrared absorption of thin metal films," Journal of Optical Society of America, V 44, n 3, pp. 188-191.

HOWELLS, G.
1954 "Measurement of plating thickness," Journal of Corrosion Technology, V 1, n 7, pp. 233-236.

IRON AND STEEL INSTITUTE
1931 "The first report of the corrosion committee," Published at the Office of the Iron and Steel Institute, London.

JELINEK, R. V.
1959 "Correlate corrosion testing methods," Chemical Engineering, V. 66, n 2, pp. 105-110.

KNAPP, B. B.
1948 "Preparation and cleaning of samples," A paper pp. 1077-1083, in H. H. Uhlig, ed. The Corrosion Handbook. John Wiley and Sons, Inc., New York, 1188 pp.

KELLY, J. C.
1958 "The interferometric measurement of metal oxide films," Optica Acta, V 5, n 3-4, pp. 75-78.

LEBERKNIGHT, C. E. and B. LUSTMAN
1939 "An optical investigation of oxide films on metals," Journal of Optical Society of America, V 29, n 2, pp. 59-66.

McCOLLAM, C. H. and D. L. WARRICK
1948 "The pickling of iron and steel products," A paper, pp. 725-729, in Taylor Lyman ed. Metals Handbook. The American Society for Metals. Cleveland, 1444 pp.

McMASTER, W. D.
1956 "Accelerated testing of metallic surfaces. The salt spray test and its modifications," Metal Finishing, V 54, n 11, pp. 48-51 and 55.

MEYER, W. R.
1948 "Solvent and vapor cleaning of metals," A paper pp. 299-300, in Taylor Lyman ed. Metals Handbook. The American Society for Metals, Cleveland, 1444 pp.

MORSE, R. N. and R. V. DUNKLE
1962 "Solar energy as an aid to the development of tropics," Sixth World Power Conference, Paper 119 III 7/2. Sub-division III 7, V 8, pp. 3084-3102.

MULVANEY, T. R.
1962 "Corrosion of mild steel in alkaline sequestering agent solutions." A Ph.D. thesis. Michigan State University, East Lansing, Michigan.

PORTEUS, J. O.
1963 "Relation between the height distribution of a rough surface and the reflectance at normal incidence," Journal of Optical Society of America, V 53, n 12, pp. 1394-1402.

SABOTKA, R.
1961 "Solar water heaters," Agenda item III C-1, United Nations Conference on New Sources of Energy.

SCOTT, G. D.
1955 "Optical constants of thin-film materials," Journal of Optical Society of America, V 45, n 3, pp. 176-178.

SENNET, R. S. and G. D. SCOTT
1950 "The structure of evaporated metal films and their optical properties," Journal of Optical Society of America, V 40, n 4, pp. 203-211.

STROUD, G.
1951 "The quantitative removal of corrosion products from zinc," Journal of Applied Chemistry, V 1, n 1, pp. 93-95.

TABOR, H., J. HARRIS, H. WEINBERGER and B. DORON
1961 "Further studies on selective black coatings," Agenda item III B, United Nations Conference on New Sources of Energy.

TANISHITA, I.
1961 "Recent developments of solar water heaters in Japan," Agenda item III C-1. United Nations Conference on New Sources of Energy.

TOLANSKY, S.
1948 Multiple Beam Interferometry. Clarendon Press, Oxford.

TROMBE, F. and M. LePHAT VINH
1961 "Studies on selective surfaces for air-conditioning dwellings," Agenda item III B. United Nations Conference on New Sources of Energy.

TRONSTAD, L.
1932 "The investigation of thin surface films on metals by means of reflected polarized light," Transactions of Faraday Society, V 28, pp. 502-514.

TRONSTAD, L.
1935 "The validity of Drude's optical method of investigating transparent films on metals," Transactions of Faraday Society, V 31, pp. 1151-1158.

UHLIG, H. H. (ed.)
1948 Corrosion Handbook. John Wiley and Sons, Inc., New York.

UHLIG, H. H.
1963 Corrosion and Corrosion Control. John Wiley and Sons, Inc., New York.

VERMILYEA, D. A.
1953 "The kinetics of formation and structure of anodic oxide films on tantalum," Acta Metallurgica, V 1, n 5, pp. 282-294.

VERNON, W. H.
1927 "Second experimental report to the atmospheric corrosion research committee (British Non-ferrous Metals Research Association), Transactions of Faraday Society, V 23, pp. 113-204.

VERNON, W. H.
1935 " Laboratory study of the atmospheric corrosion of metals. Part II. Iron: The primary oxide film. Part III. The secondary product or rust (Influence of sulphur dioxide, carbon dioxide and suspended particles on the rusting of iron)." Transactions of Faraday Society, V 31 part 2, pp. 1668-1700.

VOIGT, L. R.
1948 "Selected bibliography on salt spray testing 1935-46," Journal of Corrosion, V 4, n 10, pp. 492-504.

WASHBURN, E. W. (ed.)
1929 International Critical Tables of Numerical Data, Physics, Chemistry and Technology. V 5, p. 250, and V 7, p. 20. Published for the National Research Council by the McGraw-Hill Book Co., Inc., New York.

WEAST, R. C. and S. L. SHULMAN
1962 "Corrosion of zinc in pressurized dilute aqueous solution system," Journal of Corrosion, V 18, n 11, pp. 417-418.

WESLEY, W. A.
1943 "The total corrosion immersion test," Proceedings of the American Society for Testing Materials, V 43, pp. 649-658.

WILLIAMS, E. C. and P. C. S. HAYFIELD
1957 "Point defects near the surface of a metal," Institute of Metals Monograph no. 23, pp. 131-157.

WINTERBOTTOM, A. B.
1946 "Optical methods of studying films on reflecting bases depending on polarization and interference phenomena," Transactions of Faraday Society, V 42, pp. 487-495.

APPENDIX

Table 1. Thickness of oxide films on zinc and galvanized steel samples measured by (a) the weight change method and (b) the metallographic method

Sample No.	Exposure Duration	Oxide Film Thickness, Microns			
		Zinc		Galvanized Steel	
		(a)	(b)	(a)	(b)
Atmospheric Test					
9	3 days	1.2	1.1	1.4	1.4
10	1 week	1.9	1.8	1.7	1.6
11	2 weeks	2.7	2.5	1.9	1.8
12	3 "	3.2	3.0	2.4	2.2
1d	4 "	3.2	3.1	2.8	2.6
2d	6 "	3.2	3.0	2.9	2.8
3d	8 "	3.3	3.2	3.4	3.2
4d	12 "	3.5	3.3	4.1	3.8
Cabinet Test					
16	¼ day	1.5	1.3	4.3	3.8
15	½ day	2.4	2.2	4.0	3.7
14	1 "	5.5	4.8	6.0	5.5
13	2 days	6.6	6.0	10.8	9.3
5d	3 "	6.0	5.1	11.4	9.8
6d	5 "	6.6	5.9	9.4	8.4
7d	9 "	7.1	7.0	10.9	10.3
8d	14 "	7.9	6.8	7.1	6.7
9d	21 "	8.7	7.4	10.0	8.5
10d	28 "	8.8	7.3	12.6	10.4

Table 2. Measured r.m.s. surface roughness values (in microns) of (a) clean surface, (b) oxidized surface, and (c) metal surface after removal of oxide

	Zinc			Galvanized Steel		
Sample No.	(a)	(b)	(c)	(a)	(b)	(c)
Atmospheric Test						
9	.13	.20	.18	.28	.36	.33
10	.12	.38	.28	.25	.61	.51
11	.14	.56	.31	.22	.56	.53
12	.10	.43	.31	.28	.71	.56
1d	.10	.46	.33	.26	.89	.66
2d	.12	.38	.31	.26	.84	.64
3d	.11	.33	.31	.22	.89	.64
4d	.13	.38	.33	.25	.89	.58
Cabinet Test						
16	.14	.41	.31	.26	.64	.38
15	.10	.76	.46	.26	.58	.33
14	.13	1.40	.46	.28	.58	.33
13	.11	1.52	.71	.30	2.79	.89
5d	.11	1.27	.46	.20	.89	.66
6d	.12	1.52	.64	.25	1.78	.76
7d	.14	1.40	.51	.28	3.30	.86
8d	.12	1.91	.56	.30	2.29	1.02
9d	.13	1.91	.76	.27	3.05	1.02
10d	.10	2.54	.76	.29	4.45	1.14

Table 3. Experimental values of mean integrated hemispherical reflectance

	Zinc		Galvanized Steel	
Sample No.	3000°R Source	10,000°R Source	3000°R Source	10,000°R Source
Atmospheric Test				
9	.781	.534	.699	.470
10	.723	.440	.694	.429
11	.679	.395	.672	.391
12	.689	.383	.658	.359
1d	.711	.420	.693	.394
2d	.714	.417	.696	.394
3d	.666	.393	.676	.389
4d	.651	.373	.645	.350
Cabinet Test				
16	.687	.514	.705	.472
15	.643	.448	.645	.391
14	.626	.423	.594	.373
13	.610	.408	.504	.361
5d	.524	.317	.509	.301
6d	.558	.332	.564	.320
7d	.578	.351	.523	.313
8d	.574	.353	.648	.380
9d	.566	.353	.593	.354
10d	.551	.349	.496	.335

Table 4. Spectral values of optical constants of zinc and zinc oxide (International Critical Tables, Volume V, p. 250 and Volume VII, p. 20)

Zinc			Zinc Oxide	
Wavelength Microns	Refractive Index n	Extinction Coefficient k	Wavelength Microns	Refractive Index n
0.257	0.55	1.10	0.434	2.1395
0.275	0.46	2.56	0.436	2.1358
0.298	0.47	3.41	0.447	2.1143
0.326	0.60	3.72	0.471	2.0806
0.361	0.72	3.63	0.486	2.0649
0.398	0.85	3.45	0.492	2.0593
0.441	0.93	3.40	0.502	2.0515
0.468	1.05	3.32	0.546	2.0228
0.508	1.41	2.92	0.589	2.0041
0.598	1.93	2.41	0.656	1.9843
0.598	2.21	2.61	0.668	1.9817
0.630	2.36	2.34	0.706	1.9740
0.668	2.62	1.94	0.768	1.9648